

# Development and analysis of a Bayesian water balance model for large lake systems

Joeseph P. Smith<sup>a</sup>, Andrew D. Gronewold<sup>b,c</sup>

<sup>a</sup>*Cooperative Institute for Great Lakes Research (CIGLR), University of Michigan, Ann Arbor, Michigan USA, 48109*

<sup>b</sup>*Great Lakes Environmental Research Laboratory, National Oceanic and Atmospheric Administration, Ann Arbor, Michigan, USA, 48108*

<sup>c</sup>*Department of Civil and Environmental Engineering, University of Michigan, Ann Arbor, Michigan USA, 48109*

---

## Abstract

Water balance models are often employed to improve understanding of drivers of change in regional hydrologic cycles. Most of these models, however, are physically-based, and few employ state-of-the-art statistical methods to reconcile measurement uncertainty and bias. Here, we introduce a framework for developing, analyzing, and selecting among alternative formulations of a statistical water balance model for large lake systems that addresses this research gap. We demonstrate our new analytical framework using a model customized for Lakes Superior and Michigan-Huron, the two largest lakes on Earth by surface area. The selected model (from among 26 alternatives) closed the water balance across both lakes and had a computation time of roughly 95 minutes — an order of magnitude less than prototype versions of the same model. We expect our new framework will be used to improve computational efficiency and skill of water balance models for other lakes around the world.

---

## Software Availability

Names of software product(s): Large Lake Statistical Water Balance Model (L2SWBM)

---

\*Corresponding author. Tel.: +1-734-741-2252, Fax: +1 734-741-2055  
Email address: [joeseph@umich.edu](mailto:joeseph@umich.edu) (Joeseph P. Smith)

Developers:

National Oceanic and Atmospheric Administration  
Great Lakes Environmental Research Laboratory  
Ann Arbor, Michigan, USA  
and

Cooperative Institute for Great Lakes Research  
University of Michigan  
Ann Arbor, Michigan, USA

Hardware required: Computer with a Windows, Apple, or Linux-based operating system and modern system specifications

Software required: R statistical programming environment, Just Another Gibbs Sampler (JAGS)

Program languages: R and BUGS

Availability: Online at <https://www.glerl.noaa.gov/data/WaterBalanceModel/>

## 1. Introduction

As global freshwater demand increases (Vörösmarty et al., 2000; Martine et al., 2008), there is a simultaneously growing need for a comprehensive understanding of changes in the hydrologic cycle and of the drivers behind those changes (Makhoul and Michel, 1994; Vörösmarty et al., 1998; Guo et al., 2002; Boughton, 2004; Kebede et al., 2006). Water balance models have often been employed to shape that understanding through numerous practical applications including water resources management decision support, and guidance on policies for consumptive use and irrigation practices (Xu and Singh, 1998; Arnell, 1999; Jin et al., 2000; Mouelhi et al., 2006; Raes et al., 2006; Li et al., 2007; Crow et al., 2008). We find, however, that most models used to quantify major components of the hydrologic cycle are physically-based, and that few employ robust state-of-the-art statistical methods to incorporate measurement uncertainty, correlation, and bias into model-based simulations (Kim and Stricker, 1996; Rodell et al., 2004; Gibson et al., 2006; Benke et al., 2008; Sheffield et al., 2009). Furthermore, few historical studies provide methodological guidance for developing and selecting a suitable water

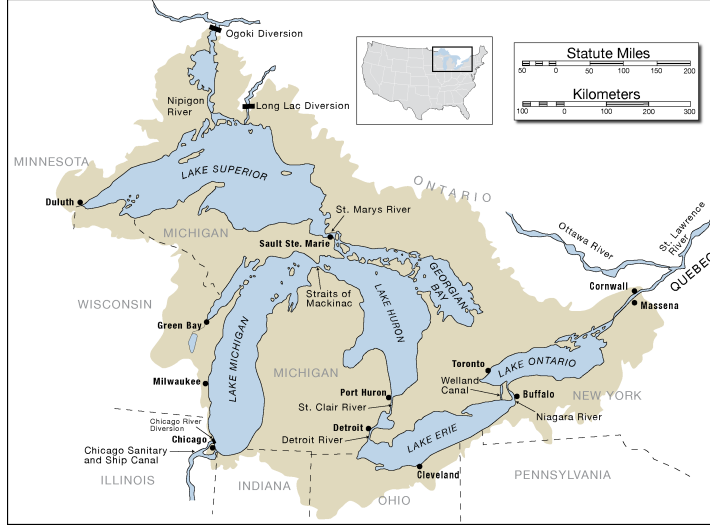


Figure 1: The Laurentian Great Lakes and their basin (light brown region) including location of major cities, interbasin diversions, and connecting channels.

balance model in light of criteria relevant to water resource management agencies, policy makers, and other model end-users.

To address these gaps, we introduce a framework for developing and analyzing alternative formulations of a Bayesian Markov chain Monte Carlo (or MCMC, for details see Gaucherel et al., 2008; Joseph and Guillaume, 2013) statistical water balance model for large lake systems, and for selecting from among those formulations using a range of conventional and non-conventional criteria (Geyer, 1992; Diaconis, 2009; Richey, 2010). We demonstrate our new analytical framework using a lake water balance model customized for Lakes Superior and Michigan-Huron (figure 1), the two largest lakes on Earth by surface area (Gronewold et al., 2013b). Over relatively coarse (e.g. monthly) time scales, Lakes Michigan and Huron are typically represented as a single lake (Lake Michigan-Huron) because they are connected by the Straits of Mackinac, and because their long-term water levels are nearly equal.

A prototype version of this lake water balance model was recently de-

veloped by Gronewold et al. (2016) to differentiate hydrologic drivers of the 2013-2014 record-setting water level rise on Lakes Superior and Michigan-Huron. While the prototype model achieved this goal, regional water resource management authorities have expressed interest in an expanded version of the model applied to all of the Laurentian Great Lakes and across a longer historical period. Before this expansion, however, two limitations in the prototype need to be addressed. The first is a long run time; preliminary results indicate that the prototype takes roughly 16 hours to simulate reliable water balance component estimates. This run time is much greater than what water management authorities are hoping for, and is particularly problematic considering that the prototype model only includes Lakes Superior and Michigan-Huron for the 120 months between 2005 to 2014.

Second, regional water resource management authorities have indicated that St. Clair River flows inferred from the prototype model are biased with an unrealistically broad range of uncertainty, and that future model development should reflect stronger *a priori* opinions about the accuracy of *in situ* measurements in the St. Clair and other connecting Rivers (also commonly referred to as “connecting channels” - Quinn and Guerra, 1986; Mueller et al., 2007). Addressing this bias is important because it may reflect unresolved uncertainties in “upstream” water balance component estimates, particularly from Lake Superior, that are being propagated downstream through the connecting channels. If unresolved, these uncertainties could, in an expanded version of the model, continue to be propagated downstream and lead to more significant biases of flow estimates in the Detroit, Niagara, and St. Lawrence Rivers (figure 1).

The primary objective of this study, therefore, is the development of a framework for systematic evaluation of alternative formulations of a statistical lake water balance model with several thousand variables and parameters. Our secondary goal is the application of this framework to the Great Lakes prototype lake water balance model to demonstrate how it can be used to improve model efficiency while incorporating *a priori* opinions about biases and uncertainties in existing data sources for components of the Great Lakes hydrologic cycle. We expect the new framework will be useful to improve large lake water balance models in other parts of the world, and that the resulting new Great Lakes water balance model, following implementation of our recommended improvements, will be suitable for deployment in operational environments and for future expansion across the entire Great Lakes system over a longer historical period.

## 2. Methods

We begin with a brief description of our lake water balance model followed by descriptions of the data, the prior probability distributions, and the likelihood functions employed in our Bayesian model formulation. We then describe our use of MCMC software to simulate samples from the posterior probability distribution for each model parameter, followed by our approach to systematically evaluating model alternatives across different performance criteria.

### 2.1. Model description

We employ a customized version of a conventional lake water balance model in which changes in lake storage across a period of  $w$  months  $\Delta H_{t,w}$  (in mm over the surface area of each lake) are defined as the difference between the lakewide-average surface water elevation at the beginning of month  $t$ , and the lakewide-average surface water elevation at the beginning of month  $t+w$  (we hereafter refer to  $w$  as the length, in months, of the water balance “rolling window”). Changes in lake storage are then related to monthly-average water balance components as follows:

$$\Delta H_{t,w} = H_{t+w} - H_t = \sum_{i=t}^{t+w-1} (P_i - E_i + R_i + I_i - Q_i + D_i + \epsilon_i) \quad (1)$$

where (all in mm over each lake surface area)  $P$  is over-lake precipitation,  $E$  is over-lake evaporation,  $R$  is lateral tributary runoff into the lake,  $I$  is inflow from an upstream connecting channel,  $Q$  is outflow to a downstream connecting channel,  $D$  represents diversions into or (expressed as a negative value) out of the lake basin, and  $\epsilon$  is a process error (Ahrestani et al., 2013) term accounting for thermal expansion, glacial isostatic rebound, ground-water fluxes, and other sources of variability in monthly water levels not explained by water balance components  $P, E, R, I, Q$ , and  $D$  alone, nor are consistently measured in terms of impact on water level. As described in greater detail in section 2.3, alternative formulations for process error  $\epsilon$  and for the length of the rolling window  $w$  represent the first two factors of our experimental design.

We apply our water balance model (equation 1) to both Lakes Superior and Michigan-Huron. When applied to Lake Superior,  $I = 0$  because Lake

Superior is the most “upstream” of the Laurentian Great Lakes and there is no inflow from a connecting channel. There are, however, interbasin diversions (i.e. the Ogoki and Long Lac diversions; see figure 1) into the Lake Superior basin. Similarly, when applied to Lake Michigan-Huron,  $I$  is defined as a linear function (to account for the difference between the surface areas of Lakes Superior and Michigan-Huron) of outflow from Lake Superior to explicitly represent inter-lake hydrologic connectivity through the St. Marys River (figure 1).

## 2.2. Model inference

We infer values for each component of each lake’s monthly water balance, along with the other model parameters, in a Bayesian framework (Gelman and Rubin, 1992; Malve et al., 2007; Dorner et al., 2007). In the following subsections, we begin by describing the data available for our Bayesian models. We then provide a description of our prior probability distribution and likelihood functions, followed by a description of our implementation of Gibbs sampling for estimating parameters’ posterior probability distributions.

### 2.2.1. Data

Data for estimating parameters of prior probability distributions and for populating likelihood functions are available from a variety of sources (table 1), including the National Oceanic and Atmospheric Administration Great Lakes Environmental Research Laboratory (NOAA-GLERL) Great Lakes Monthly Hydrometeorological Database (or GLM-HMD, described in Hunter et al., 2015), as well as legacy datasets of lakewide average water levels, channel flows, and diversions from the Coordinating Committee on Great Lakes Basic Hydraulic and Hydrologic Data (CCGLBHHD). They also include newer data sets either developed by Environment and Climate Change Canada (ECCC) or (e.g. for connecting channel flows) adapted from gauging stations maintained through a binational partnership between the United States and Canada. For further reading on the historical development and application of these datasets, see Gronewold et al. (2016) as well as the references identified in table 1.

### 2.2.2. Prior probability distributions and likelihood functions

We develop a distinct prior probability distribution for each water balance component for each month of the year by (following Gronewold et al., 2016)

Variable	Data source description	Year range used for prior probability distribution	Year range used for likelihood function	Reference
$y_{\Delta H}$	CCGLBHHD	NA	2005-2014	CCGLBHHD (1977)
$y_{P,1}$	GLM-HMD	1950-2004	2005-2014	Hunter et al. (2015)
$y_{P,2}$	GEM-MESH w/CaPA	NA	2005-2014	Lespinas et al. (2015)
$y_{E,1}$	GLM-HMD (LLTM)	1950-2004	2005-2014	Hunter et al. (2015)
$y_{E,2}$	GEM-MESH	NA	2005-2014	Deacu et al. (2012)
$y_{R,1}$	GLM-HMD (ARM)	1950-2004	2005-2014	Hunter et al. (2015)
$y_{R,2}$	NOAA-GLERL LBRM	NA	2005-2014	Croley and He (2005)
$y_{Q,1}$	CCGLBHHD	1950-2004	2005-2014	CCGLBHHD (1977)
$y_{Q,2}$	IGS	NA	Nov. 2008-2014	United States Geological Survey (2017)
$y_{D,1}$	CCGLBHHD	1950-2004	2005-2014	CCGLBHHD (1977)

Table 1: Summary of data sets used to develop water balance component prior probability distributions and as a basis for likelihood functions. International gauging stations (IGS) used in this study are located at Sault Ste. Marie (for outflows from Lake Superior) and Port Huron (for outflows from Lake Michigan-Huron) and are maintained through a partnership between the United States Geological Survey (USGS) and Water Survey of Canada. Measurements of diversions into (or out of) each lake basin ( $y_{D,1}$ ) include the Ogoki River and Long-Lac diversions into Lake Superior, and the Chicago diversion out of Lake Michigan-Huron. CCGLBHHD refers to the Coordinating Committee on Great Lakes Basic Hydraulic and Hydrologic Data, an ad hoc group of science agencies from both the United States and Canada. For other acronyms and abbreviations, see the references listed.

empirically fitting probability density functions to historical water balance data from the NOAA-GLERL GLM-HMD and the CCGLBHHD (table 1) between 1950 and 2004 (see supplementary material for related figures). Because the range of historical values of evaporation ( $E$ ) and channel outflows ( $Q$ ) is quite narrow for certain months of the year, we doubled the variance of the prior probability distributions for these two variables to reflect the possibility that they might evolve over time beyond the limits of that historical range due to changes in climate and other factors (Milly et al., 2008). We do not expect empirically-derived prior probability distributions for other, more intrinsically variable water balance components to restrict evolution of their respective posterior probability distributions.

We then employ the following likelihood functions for observed changes in storage from January 2005 through December 2014:

$$y_{\Delta H,t,w} \sim \mathcal{N}(\Delta H_{t,w}, \sigma_{y,\Delta H}^2) \quad (2)$$

with a non-informative inverse-gamma  $\text{IG}(0.01, 0.01)$  prior on variance  $\sigma_{y,\Delta H}^2$ . For components of the water balance, we employ normal  $\mathcal{N}(\mu, \sigma^2)$  likelihood functions (for data from January 2005 through December 2014) where the observed value of component  $\theta_t$  from data source  $n$  ( $y_{\theta,n,t}$ ) is related to the true value of  $\theta_t$  as:

$$y_{\theta,n,t} \sim \mathcal{N}(\theta_t + \eta_{\theta,n,t}, \sigma_{y,\theta,n}^2), \theta \in (P, E, R, Q, D) \quad (3)$$

with  $\eta_{\theta,n,t}$  representing observation bias (or error), and a non-informative inverse-gamma  $\text{IG}(0.1, 0.1)$  prior on component likelihood variance  $\sigma_{y,\theta,n}^2$ . As described in greater detail in section 2.3, alternative formulations of data bias represent the third factor in our experimental design.

### 2.2.3. Bayesian Markov chain Monte Carlo (MCMC) implementation

We use MCMC methods to infer parameter values across multiple versions of our model (detailed descriptions of alternative model formulations are included in section 2.3) with JAGS (Just Another Gibbs Sampler; see Plummer et al., 2003), and the ‘rjags’ package in the R statistical software environment (R Core Team, 2014). We run JAGS for each model alternative for 250,000 iterations across three parallel MCMC chains, and thin the last 125,000 iterations of each chain (omitting the first 125,000 iterations as a

‘burn-in’ period) at even intervals such that the resulting ‘thinned’ chains each have 1,000 values. The resulting 3,000 MCMC samples (1,000 samples per chain) for each parameter then serve as the basis for our posterior probability distribution inference and overall performance assessment. We ran the models on a Windows 7 Professional (Microsoft, Redmond, WA, USA) workstation with a 64-bit Intel Core i7-3770 (3.4 GHz) processor with 32 GB of RAM. JAGS model code is included in the supplementary material.

### *2.3. Experiment design*

We formally analyzed alternative configurations of our lake water balance model using a modified factorial experiment design (Montgomery, 2008) across three experimental variables (table 2) including the length of the rolling water balance window  $w$ , the prior probability distribution on process error  $\pi(\epsilon)$ , and the prior probability distribution on observation bias  $\pi(\eta)$ .

For the length of the rolling water balance window  $w$ , we consider three alternatives. The first follows the approach employed in the prototype model, as a basis for comparison, in which the water balance model is resolved across incrementally increasing time steps starting with a one month time step, and ending with a  $T$  month time step (where  $T=120$  is the total number of months in our study). Our second and third alternatives are rolling windows of 1 and 12 months, respectively, and are intended to simultaneously reduce model computational time relative to the prototype model while assessing the impact of different rolling window lengths on water balance estimates (e.g. monthly, seasonal, and inter-annual scales) relevant to regional water resource management decisions.

We then consider three formulations ( $\epsilon_A$ ,  $\epsilon_B$ ,  $\epsilon_C$ ) of the prior probability distribution for process error  $\epsilon$ . The first, following the prototype, is a model in which there is no explicit process error term ( $\epsilon_A = 0$ ) and unexplained variability in observed changes in storage propagates into water level measurement uncertainty through  $\sigma_{y,\Delta H}^2$  (equation 2). The second alternative prior for process error is based on a fixed, diffuse prior with a mean of zero for each of the 12 calendar months,  $c(t)$ , to track potential seasonality of process error:

$$\epsilon_{B,t} = \epsilon_{B,c(t)} \sim N(0, 100) \quad (4)$$

The third and final alternative is more relaxed, allowing for unique, monthly

process errors via a hierarchical structure. Each month's process error is given a prior with a calendar month-specific mean,  $\epsilon_{C,c(t)}$ , and variance,  $\sigma_{\epsilon,c(t)}^2$ :

$$\begin{aligned}\epsilon_{C,t} &\sim \mathcal{N}(\epsilon_{C,c(t)}, \sigma_{\epsilon,c(t)}^2) \\ \epsilon_{C,c(t)} &\sim \mathcal{N}(0, 100) \\ \sigma_{\epsilon,c(t)}^2 &\sim \text{IG}(0.05, 0.05)\end{aligned}\tag{5}$$

Both  $\epsilon_B$  and  $\epsilon_C$  are intended to isolate water level measurement uncertainty from uncertainty in the balance model, and thus are modelled at seasonal and monthly temporal resolutions, respectively, while  $\sigma_{y,\Delta H}^2$  is assumed to be constant throughout the analysis period.

Lastly, we formally consider three alternatives for formulating prior probability distributions for the bias of data sources  $y_P$ ,  $y_E$ ,  $y_R$ ,  $y_Q$ , and  $y_D$ . The first, following equation 4 and the prototype model, is a diffuse prior for all variables (we remove subscripts  $n$  and  $\theta$  here for clarity):

$$\eta_{A,t} = \eta_{A,c(t)} \sim \mathcal{N}(0, 100)\tag{6}$$

and the second, following equation 5, is a hierarchical prior for all variables:

$$\begin{aligned}\eta_{B,t} &\sim \mathcal{N}(\eta_{B,c(t)}, \sigma_{\eta,c(t)}^2) \\ \eta_{B,c(t)} &\sim \mathcal{N}(0, 100) \\ \sigma_{\eta,c(t)}^2 &\sim \text{IG}(0.05, 0.05)\end{aligned}\tag{7}$$

We then consider a third alternative to reflect the *a priori* opinions of regional water resource management authorities regarding the accuracy of channel flow ( $Q$ ) and diversion ( $D$ ) estimates. Following informal protocols for soliciting *a priori* expert opinions (Borsuk et al., 2001; Voinov and Bousquet, 2010), we found that regional water management authorities believe that monthly channel flow data can depart from “true” channel flows by between roughly 180 and 270 cubic meters per second (cms). Over the course of a 30-day month, this flow measurement error is roughly equivalent to 6 to 9mm of water over the surface of Lake Superior, and 4 to 6mm of water over the surface of Lake Michigan-Huron. We reflect these *a priori* opinions through modified, more informative versions of equations 6:

$$\eta_{A,t}^* = \eta_{A,c(t)}^* \sim N(0, 4) \quad (8)$$

and 7:

$$\begin{aligned}\eta_{B,t}^* &\sim N(\eta_{B,c(t)}^*, \sigma_{\eta^*,c(t)}^2) \\ \eta_{B,c(t)}^* &\sim N(0, 4)\end{aligned}\quad (9)$$

For further discussion on error modelling in hydrology, see Li et al. (2013), Schoups and Vrugt (2010), Bates and Campbell (2001), and Engeland and Gottschalk (2002).

## 2.4. Model evaluation

### 2.4.1. Water balance “closure”

To be of practical use in water resource management decisions, our model-derived water balance component estimates should “close” the water balance across a range of different time periods (Pan and Wood, 2006). We assess water balance closure by simulating the posterior predictive distribution (Gelman and Shalizi, 2013; Kruschke, 2013) of measured changes in lake storage across all 1, 12, and 60-month periods ( $y'_{\Delta H,t,1}$ ,  $y'_{\Delta H,t,12}$ ,  $y'_{\Delta H,t,60}$ ) from 2005 through 2014, and then calculating the frequency with which the 95% posterior predictive intervals contain the corresponding observed changes in lake storage ( $y_{\Delta H,t,1}$ ,  $y_{\Delta H,t,12}$ ,  $y_{\Delta H,t,60}$ ). JAGS code for calculating posterior predictive distributions is included in the supplementary material.

We recognize that our model evaluation design (table 2) does not include water balance component inference using a model with a rolling window ( $w$ ) of 60 months and, furthermore, that a range of different rolling windows could have been explored for inference in our experiment design. Regardless, our approach addresses the question of whether water balance components inferred from a model with only a 1-month rolling window (which may have the advantage of a relatively short computation time) close the water balance over periods longer than one month, or if a longer rolling window (in our case, assessed using a 12-month window) is needed.

### 2.4.2. Model convergence and computation time

For each model in our experimental design, we assess the rate and extent of convergence across  $K = 250,000$  MCMC iterations by calculating the

$w$	$\pi(\epsilon_t)$	$\pi(\eta_{P,E,R})$	$\pi(\eta_{Q,D})$	Model ID
[1, ..., $T$ ]	No error term	Fixed (eq. 6)		PROT
1	(N)o error term	(F)ixed (eq. 6)		01NF
1	(N)o error term	(H)ierarchical (eq. 7)		01NH
1	(F)ixed (eq. 4)	(F)ixed (eq. 6)		01FF
1	(F)ixed (eq. 4)	(H)ierarchical (eq. 7)		01FH
1	(H)ierarchical (eq. 5)	(F)ixed (eq. 6)		01HF
1	(H)ierarchical (eq. 5)	(H)ierarchical (eq. 7)		01HH
12	(N)o error term	(F)ixed (eq. 6)		12NF
12	(N)o error term	(H)ierarchical (eq. 7)		12NH
12	(F)ixed (eq. 4)	(F)ixed (eq. 6)		12FF
12	(F)ixed (eq. 4)	(H)ierarchical (eq. 7)		12FH
12	(H)ierarchical (eq. 4)	(F)ixed (eq. 6)		12HF
12	(H)ierarchical (eq. 4)	(H)ierarchical (eq. 7)		12HH
[1, ..., $T$ ]	No error term	Fixed (eq. 7)	(eq. 8)	fPROT
1	(N)o error term	(F)ixed (eq. 6)	(eq. 8)	f01NF
1	(N)o error term	(H)ierarchical (eq. 7)	(eq. 9)	f01NH
1	(F)ixed (eq. 4)	(F)ixed (eq. 6)	(eq. 8)	f01FF
1	(F)ixed (eq. 4)	(H)ierarchical (eq. 7)	(eq. 9)	f01FH
1	(H)ierarchical (eq. 4)	(F)ixed (eq. 6)	(eq. 8)	f01HF
1	(H)ierarchical (eq. 4)	(H)ierarchical (eq. 7)	(eq. 9)	f01HH
12	(N)o error term	(F)ixed (eq. 6)	(eq. 8)	f12NF
12	(N)o error term	(H)ierarchical (eq. 7)	(eq. 9)	f12NH
12	(F)ixed (eq. 4)	(F)ixed (eq. 6)	(eq. 8)	f12FF
12	(F)ixed (eq. 4)	(H)ierarchical (eq. 7)	(eq. 9)	f12FH
12	(H)ierarchical (eq. 4)	(F)ixed (eq. 6)	(eq. 8)	f12HF
12	(H)ierarchical (eq. 4)	(H)ierarchical (eq. 7)	(eq. 9)	f12HH

Table 2: Summary of our experimental design in which alternative models are configured with variations in the length of monthly water balance window (used in model inference)  $w$ , prior probability distributions for process error  $\pi(\epsilon_t)$ , and prior probability distribution for data bias  $\pi(\eta)$ .

potential scale reduction factor (PSRF), also referred to as the Gelman-Rubin convergence statistic or  $\hat{R}$  (Gelman and Rubin, 1992), every 10,000<sup>th</sup> iteration for all model parameters. We calculate the PSRF using the `gelman.diag` function in the R package ‘CODA’ which returns both the median ( $\hat{R}_{50}$ ) and 97.5% quantile ( $\hat{R}_{97.5}$ ) of the PSRF. We assess convergence by testing whether these statistics approach (or decrease below) 1.1, per guidance from Gelman and Rubin (1992), as they evolve across MCMC iterations.

We also record the total time required for each model to generate 250,000 MCMC iterations. The model runs we execute for monitoring computation time do not include calculations for posterior predictive distributions (described in the previous section) because they serve as a basis for model verification only and would not, we believe, be encoded in a future version employed in routine operations.

### 3. Results and discussion

#### 3.1. Analysis of water balance closure

Our analysis of 95% posterior predictive intervals for simulated changes in lake storage across 1, 12, and 60-month periods (table 3) indicates that most models conditioned on changes in storage across a 1-month window close the water balance for Lakes Superior and Michigan-Huron in simulations over a 1-month period, but do not effectively close the water balance in simulations over 12 and 60-month periods. Water balance component estimates conditioned on a rolling 12-month storage window, however, close the water balance for 12- and 60-month periods for Lakes Superior and Michigan-Huron, and come close to closing the water balance for both lakes on a 1-month storage window. For example, 95% posterior predictive intervals for monthly changes in storage derived from 12-month rolling window models included between 91% and 100% of the observed monthly changes in storage for Lake Superior, and between 79% and 98% of observed monthly changes in storage for Lake Michigan-Huron. Similarly, 95% posterior predictive intervals for 12- and 60-month changes in storage derived from 12- month rolling window models contained 97% to 100% of the observed monthly changes in storage for both Lakes Superior and Michigan-Huron.

Our results show slight improvements in balance closure occur through either a) the introduction alone of an explicit process error term or b) the relaxation of prior probability distributions for the bias of data sources via

the introduction of a hierarchical structure. Applying a reduced range of potential bias in channel flow measurements yielded mixed results in terms of improving balance closure in a model. Models that inferred changes in storage over a 1-month window exhibited little impact on 1-month window closure rates post-application, in contrast to a maximum 17% drop (01NH to f01NH) post-application for 12 and 60 month closure rates. 12-month rolling window models were more robust, with the only decreases in performance occurring with 1-month changes in storage on Michigan-Huron — the percentage of observed changes in lake storage within 95% posterior predictive credible intervals dropped between 2% and 11% after application.

A visual inspection of a representative time series (from the f01FF and f12FF models) comparing observed and simulated changes in storage over 1, 12, and 60-month periods (figure 2) underscores the degradation in skill when water balance components inferred from a 1-month window model are used to simulate changes in lake storage across longer time periods. The visual inspection of the representative time series also indicates that while the percentage of observations within the 95% posterior predictive interval for the f12FF model (right column, figure 2) exceeds 95% when used to simulate 12- and 60-month cumulative changes in storage, overdispersion does not appear to be a significant problem. Models that infer over narrower windows allow more freedom in the exploration of values for components in a given month. Due to a lack of information from other months, however, it is difficult to close the balance over longer time periods with those models. Wider windows for inference, however, shrink the range of possible values of water balance components, as the values must close a larger number of  $w$  month balance periods.

### *3.2. Model convergence and computation time*

Results of our convergence analysis (figures 3 and 4) indicate that most models approached convergence within 250,000 iterations, but that at least one of the several thousand parameters in each of our experimental models (represented by the maximum PSRF) did not fully converge. Close inspection of these results (figures 5 and 6) indicates that, for under half the models, only a few of the parameters in each model have a PSRF above 1.1. Models with about 4000 variables, a hierarchical data source bias structure, or a combination of 1) a 12-month rolling window for inference of changes in storage and 2) hierarchical process error and bias structure, had large quantities of variables not converge. We found it most common, with models that nearly

Simulation with rolling window (months) of:						
	1		12		60	
	SUP	MHU	SUP	MHU	SUP	MHU
NULL	98	98	99	100	100	100
01NF	97	99	27	29	21	15
01NH	98	100	35	38	21	23
01FF	97	99	28	50	25	26
01FH	99	100	39	52	25	34
01HF	100	100	51	79	30	38
01HH	100	100	55	74	41	38
12NF	92	85	99	100	100	97
12NH	95	84	100	100	100	100
12FF	98	88	99	100	100	97
12FH	98	92	100	100	100	100
12HF	93	92	100	100	100	100
12HH	98	98	100	100	100	100
fNULL	98	98	99	100	100	98
f01NF	98	98	24	17	13	7
f01NH	98	99	29	21	13	13
f01FF	98	99	28	39	23	23
f01FH	99	100	35	50	21	30
f01HF	100	100	45	75	25	36
f01HH	100	100	50	76	28	38
f12NF	91	79	100	100	100	97
f12NH	95	79	100	100	100	98
f12FF	98	86	99	100	100	97
f12FH	98	88	100	100	100	100
f12HF	95	88	100	100	100	100
f12HH	100	87	100	100	100	100

Table 3: Percent (%) of observed changes in lake storage within 95% posterior predictive intervals of model-simulated changes in storage across 1, 12, and 60 month periods for Lakes Superior (SUP) and Michigan-Huron (MHU).

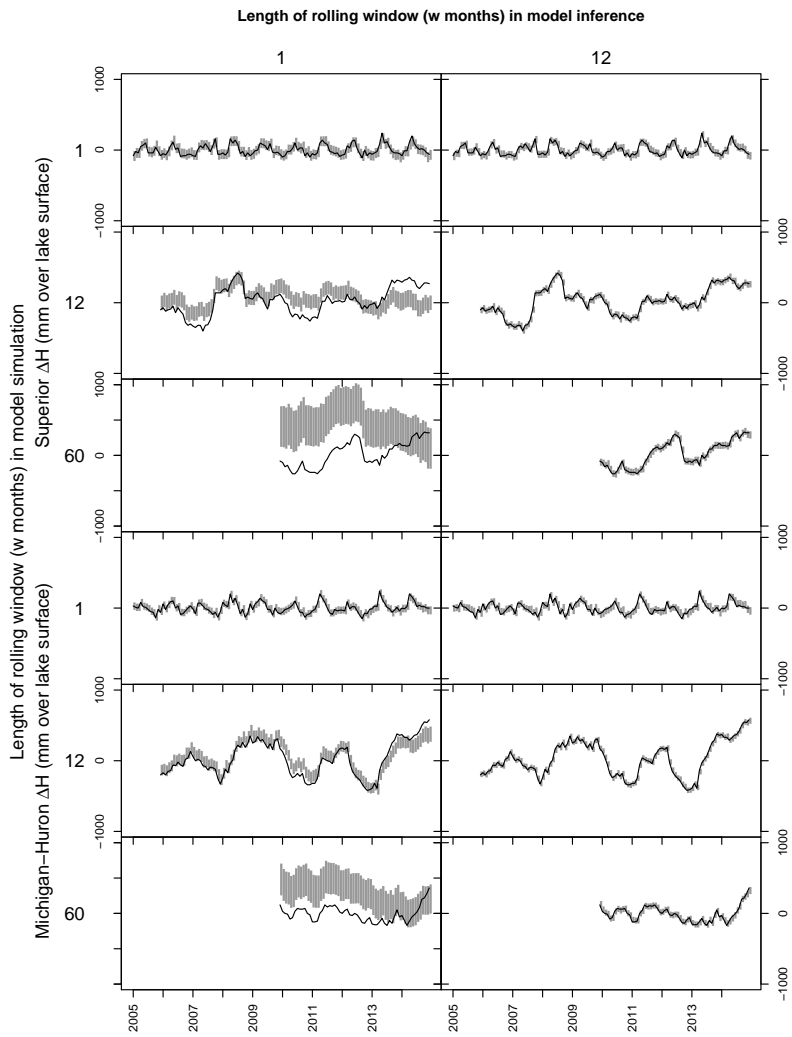


Figure 2: Comparison between observed (black line) and simulated (95% posterior predictive intervals; grey regions) changes in lake storage across a period of 1, 12, and 60 months for Lakes Superior (top three rows) and Michigan-Huron (bottom three rows). Simulated changes are based on water balance components inferred using either a 1-month (left column) or 12-month (right column) window. Simulation results shown are based on the f01FF and f12FF models (per table 3).

converged, for water balance component observation variance(s)  $\sigma_{y,\theta,n}^2$  to be the parameter(s) that did not converge (for further reading, see Brooks and Gelman, 1998).

We also find that the time to run a model (to 250,000 iterations) with a 12-month rolling inference window (also figures 3 and 4) is roughly 14 hours less than the time required for the prototype model, but roughly three times longer than the time to run a model with a 1-month inference window. The time required to run models with different process error structures are about equal, while implementing a hierarchical structure for data source bias adds up to 10 minutes compared with a fixed structure. These run times are dependent on the technical specifications of the computer used, as well as other applications being run simultaneously on the same computer. Run times will, therefore, likely differ across different computational environments.

### *3.3. Incorporating expert opinions on channel flow bias*

Reducing the *a priori* range of potential bias in channel flow measurements significantly reduced the uncertainty and central tendency of our inferred channel flow estimates (figure 7) relative to the prototype model without significantly impacting variability and bias in the other inferred water balance components (table 4). For example, we find that uncertainty in inferred water balance components (based on the width of corresponding 95% credible intervals) increased by no more than 1 to 2 mm from the prototype model to the f12FF model. In general, these results indicate that a new version of the model (e.g. f12FF, f12NF) is capable of reproducing the desirable features of the prototype model while significantly reducing model computation time (through a shorter model inference window) and reducing uncertainty in connecting channel flow estimates. Plots of time series of inferred water balance components from the prototype, model f12NF, and model f12FF are included in the supplementary material.

### *3.4. Model selection*

Our experiment indicates that month-to-month water balance inference, or inference using only a one month rolling window, does not close the balance over longer time periods. It also indicates MCMC convergence is greatly hindered, if not prevented, given a more complex hierarchical process error or component observation bias structure. Therefore, two model options can be recommended: f12NF and f12FF. Both options have a 12-month rolling

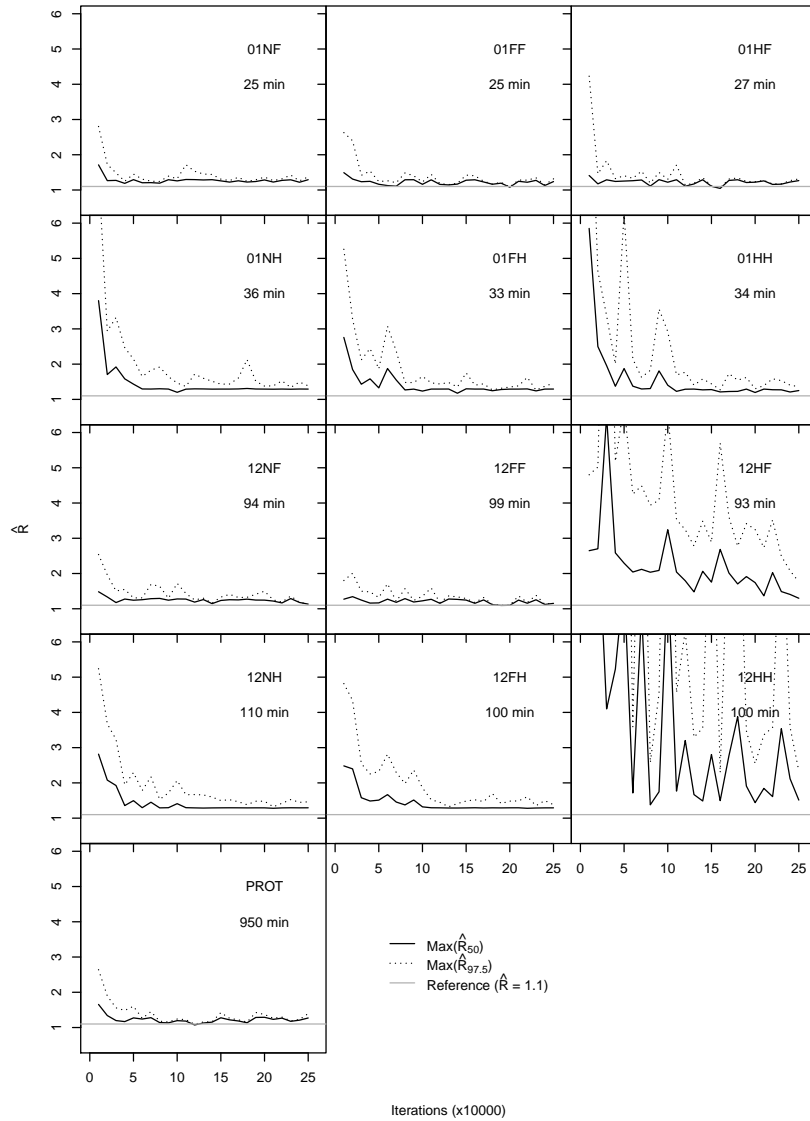


Figure 3: Evolution of the maximum value of  $\hat{R}_{50}$  and  $\hat{R}_{97.5}$  (from all parameters in a given model) across JAGS sampling iterations for models with diffuse prior probability distributions on channel flow and diversion estimate bias. Run times are beneath the model label in each panel.

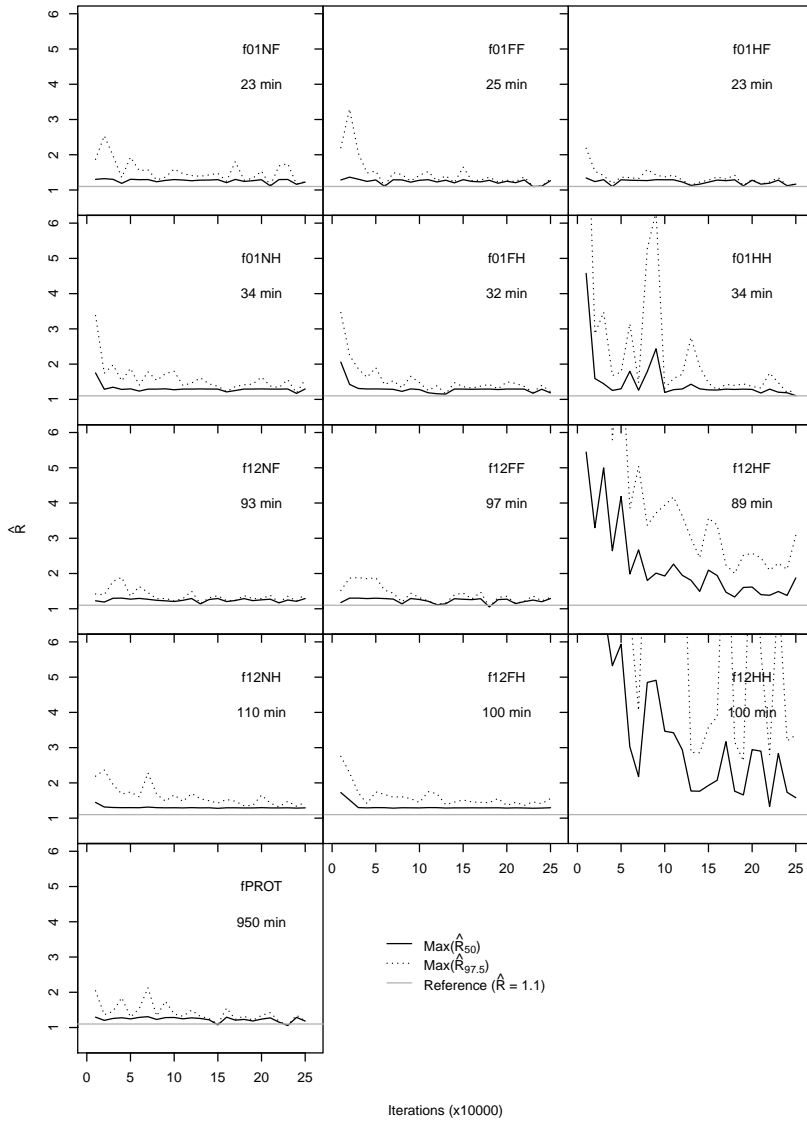


Figure 4: Evolution of the maximum value of  $\hat{R}_{50}$  and  $\hat{R}_{97.5}$  (from all parameters in a given model) across JAGS sampling iterations for models with informative prior probability distributions on channel flow and diversion estimate bias. Run times are beneath the model label in each panel.

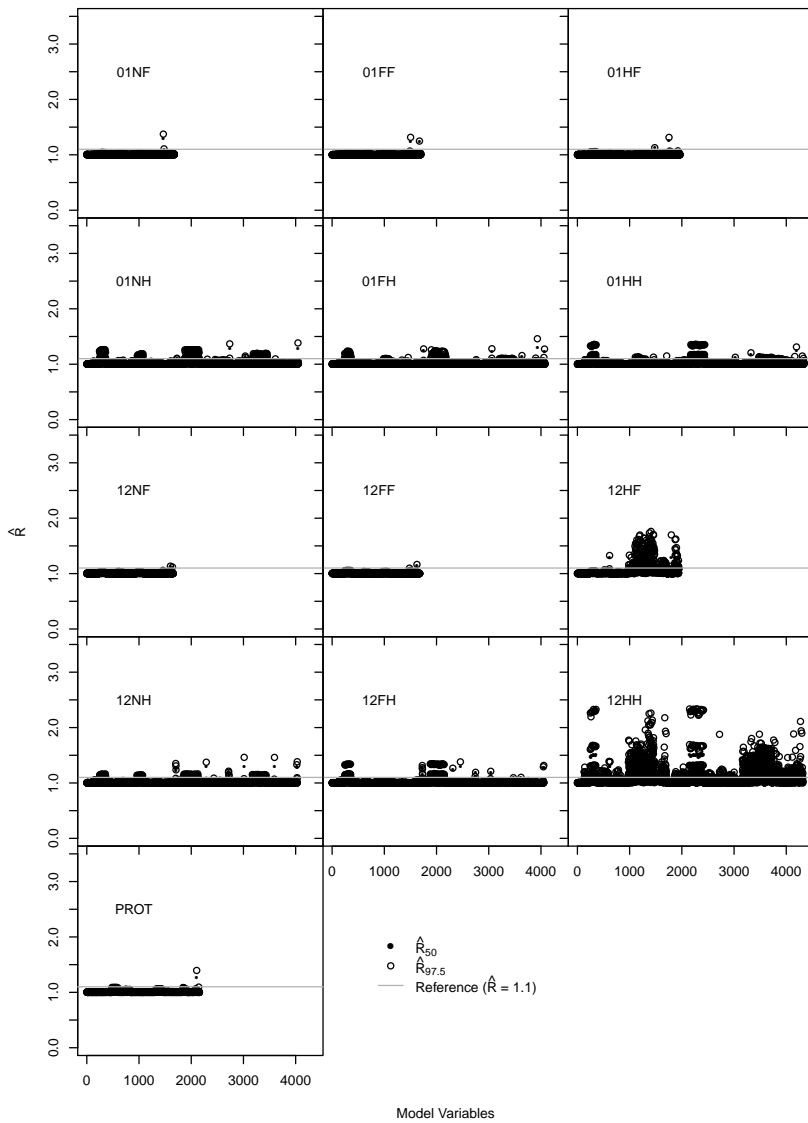


Figure 5: Analysis of PSRF for all variables of models with diffuse prior probability distributions on channel flow and diversion estimate bias (calculated after 250,000 iterations). The horizontal axis represents individual variables as well as the total quantity of variables in each model.

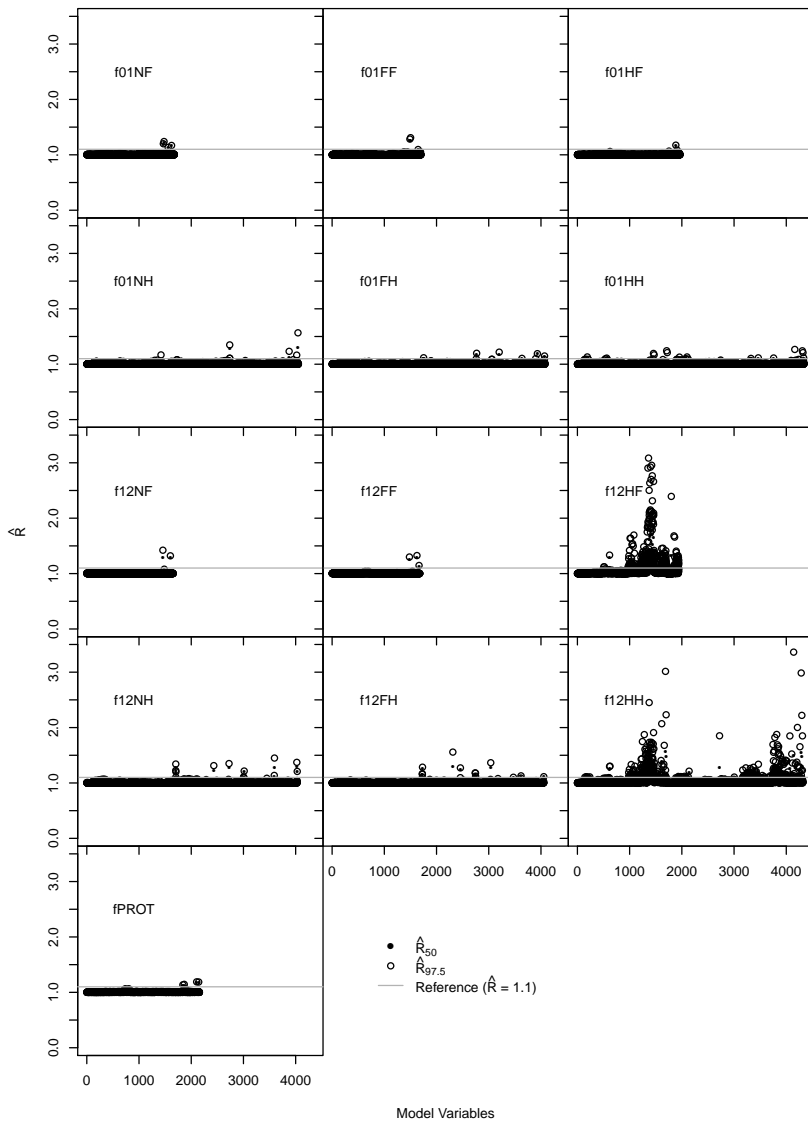


Figure 6: Analysis of PSRF for all variables of models with informative prior probability distributions on channel flow and diversion estimate bias (calculated after 250,000 iterations). The horizontal axis represents individual variables as well as the total quantity of variables in each model.

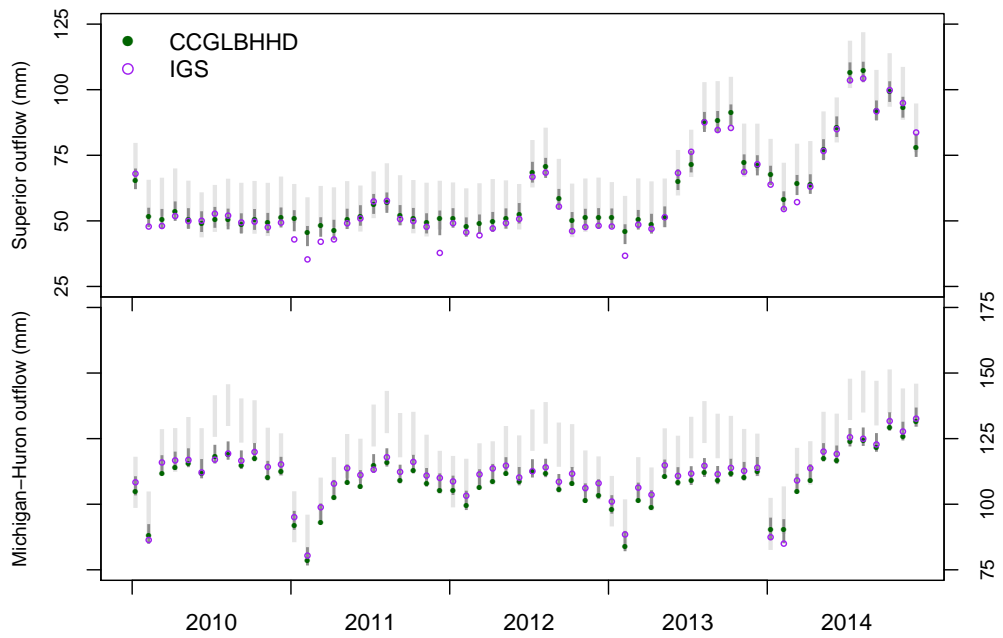


Figure 7: Estimates (95% credible intervals) of flow (in mm over the respective lake surface) through the connecting channels from Lake Superior (i.e. St. Marys River) and from Lake Michigan-Huron (i.e. St. Clair River) from the prototype model (light grey bars) and new model f12FF (dark grey bars). Historical flow measurements are represented by solid green dots (CCGLBHHD) and purple circles (IGS).

Lake and Variable	PROT	f12FF	f12NF
Superior $P$	28	29	28
Superior $E$	20	20	20
Superior $R$	19	20	20
MI-Huron $P$	26	28	28
MI-Huron $E$	19	21	21
MI-Huron $R$	18	19	18

Table 4: Comparison between the average width of 95% credible intervals (CI) for inferred values of  $P$ ,  $E$ , and  $R$  from the prototype (PROT) model and the f12FF model.

water balance window, a fixed data source bias structure as in the prototype model, and constrained priors on bias for channel flow and diversion estimates. Whether or not process error is explicitly estimated on a seasonal basis is the difference between the two options, where the advantage in the former, or f12FF, is 7% more months with a closed water balance on a monthly basis.

#### 4. Conclusions

The experiment described in this paper led to the evolution of a large lake water balance model for the Laurentian Great Lakes, and has the potential to support the development of similar models for other large lake systems around the world. In particular, our experiment evaluated impacts of the length of a model inference window, the structure of the process error, and formulation of observation bias on model convergence and computation time, as well the rate at which inferred components of the water balance closed the balance as observed through changes in water level. The experiment design can be modified to experiment with other inference windows and error structures.

Based on the above criteria and the results of the formal experiment, we recommend either f12FF or f12NF for future expansion across the other Great Lakes and for a longer period of record. Both models required roughly 1.5 hours to compute 250,000 MCMC iterations (and came close to converging after roughly 200,000 iterations), closed the water balance over 1, 12,

and 60 month periods, and incorporate current opinions of regional water management authorities. These results give water resource managers and analysts flexibility in choosing to estimate process error, which may estimate the collective impact of groundwater fluxes, isostatic rebound, thermal expansion, and other unmeasured phenomena. Expansion of the new model (or models) to Lakes St. Clair, Erie, and Ontario, as well as back in time to 1950, is expected to be non-trivial. The number of parameters to estimate will increase, and there will be other factors to consider, such as water flow through the Huron to Erie Corridor, and meteorological station and stream gauge availability over time. As the models are tested and improved, we expect that the resulting water balance component estimates will be employed not only by water management authorities, but will be distributed to the public as well through (among other interfaces) the NOAA Great Lakes Dashboard Project (Gronewold et al., 2013a; Clites et al., 2014; Smith et al., 2016).

## 5. Supplementary material

Supplementary material related to this article can be found on-line.

## 6. Acknowledgements

The authors thank Song Qian, Yves Atchade, Kerby Shedden, Edward Ionides, Vincent Fortin, Bryan Tolson, and Craig Stow for helpful discussions on Bayesian inference and alternative formulations of our water balance model. Jacob Bruxer, Frank Seglenieks, Tim Hunter, and Lauren Fry provided expert opinions and water balance data. Nicole Rice provided graphical and editorial support. Funding was provided by the International Joint Commission (IJC) International Watersheds Initiative (IWI) to NOAA and the Cooperative Institute for Great Lakes Research (CIGLR) through a NOAA Cooperative Agreement with the University of Michigan (NA12OAR4320071); many thanks to Wendy Leger and Mike Shantz. The use of product names, commercial and otherwise, in this paper does not imply endorsement by NOAA, NOAA-GLERL, CIGLR, or any other contributing agency or organization. This is NOAA-GLERL contribution number XXXX and CIGLR contribution number ZZZZ.

## References

- Ahrestani, F. S., Hebblewhite, M., Post, E., 2013. The importance of observation versus process error in analyses of global ungulate populations. *Scientific reports* 3, 3125.
- Arnell, N. W., 1999. A simple water balance model for the simulation of streamflow over a large geographic domain. *Journal of Hydrology* 217 (3), 314–335.
- Bates, B. C., Campbell, E. P., 2001. A markov chain monte carlo scheme for parameter estimation and inference in conceptual rainfall-runoff modeling. *Water resources research* 37 (4), 937–947.
- Benke, K. K., Lowell, K. E., Hamilton, A. J., 2008. Parameter uncertainty, sensitivity analysis and prediction error in a water-balance hydrological model. *Mathematical and Computer Modelling* 47 (11), 1134–1149.
- Borsuk, M. E., Clemen, R., Maguire, L., Reckhow, K. H., 2001. Stakeholder values and scientific modeling in the Neuse River watershed. *Group Decision and Negotiation* 10 (4), 355–373.
- Boughton, W., 2004. The Australian water balance model. *Environmental Modelling & Software* 19 (10), 943–956.
- Brooks, S. P., Gelman, A., 1998. General methods for monitoring convergence of iterative simulations. *Journal of Computational and Graphical Statistics* 7 (4), 434–455.
- CCGLBHHD, 1977. Coordinated Great Lakes physical data. Tech. rep., Coordinating Committee on Great Lakes Basic Hydraulic and Hydrologic Data.  
URL [www.lre.usace.army.mil/](http://www.lre.usace.army.mil/)
- Clites, A. H., Smith, J. P., Hunter, T. S., Gronewold, A. D., 2014. Visualizing relationships between hydrology, climate, and water level fluctuations on Earth's largest system of lakes. *Journal of Great Lakes Research* 40 (3), 807–811.
- Croley, T. E., He, C., 2005. Distributed-parameter large basin runoff model. I: Model development. *Journal of Hydrologic Engineering* 10 (3), 173–181.

- Crow, W. T., Kustas, W. P., Prueger, J. H., 2008. Monitoring root-zone soil moisture through the assimilation of a thermal remote sensing-based soil moisture proxy into a water balance model. *Remote Sensing of Environment* 112 (4), 1268–1281.
- Deacu, D., Fortin, V., Klyszejko, E., Spence, C., Blanken, P. D., 2012. Predicting the net basin supply to the Great Lakes with a hydrometeorological model. *Journal of Hydrometeorology* 13 (6), 1739–1759.
- Diaconis, P., 2009. The Markov chain Monte Carlo revolution. *Bulletin of the American Mathematical Society* 46 (2), 179–205.
- Dorner, S., Shi, J., Swayne, D., 2007. Multi-objective modelling and decision support using a Bayesian network approximation to a non-point source pollution model. *Environmental Modelling & Software* 22 (2), 211–222.
- Engeland, K., Gottschalk, L., 2002. Bayesian estimation of parameters in a regional hydrological model. *Hydrology and Earth System Sciences Discussions* 6 (5), 883–898.
- Gaucherel, C., Campillo, F., Misson, L., Guiot, J., Boreux, J.-J., 2008. Parameterization of a process-based tree-growth model: comparison of optimization, MCMC and particle filtering algorithms. *Environmental Modelling & Software* 23 (10), 1280–1288.
- Gelman, A., Rubin, D. B., 1992. Inference from iterative simulation using multiple sequences. *Statistical Science* 7 (4), 457–472.
- Gelman, A., Shalizi, C. R., 2013. Philosophy and the practice of Bayesian statistics. *British Journal of Mathematical and Statistical Psychology* 66 (1), 8–38.
- Geyer, C. J., 1992. Practical Markov chain Monte Carlo. *Statistical Science* 7 (4), 473–483.
- Gibson, J., Prowse, T., Peters, D., 2006. Hydroclimatic controls on water balance and water level variability in Great Slave Lake. *Hydrological Processes* 20 (19), 4155–4172.
- Gronewold, A. D., Bruxer, J., Durnford, D., Smith, J. P., Clites, A. H., Seglenieks, F., Qian, S. S., Hunter, T. S., Fortin, V., 2016. Hydrological

- drivers of record-setting water level rise on Earth's largest lake system. *Water Resources Research* 52 (5), 4026–4042.
- Gronewold, A. D., Clites, A. H., Smith, J. P., Hunter, T. S., 2013a. A dynamic graphical interface for visualizing projected, measured, and reconstructed surface water elevations on the Earth's largest lakes. *Environmental Modelling and Software* 49, 34–39.
- Gronewold, A. D., Fortin, V., Lofgren, B. M., Clites, A. H., Stow, C. A., Quinn, F. H., 2013b. Coasts, water levels, and climate change: A Great Lakes perspective. *Climatic Change* 120 (4), 697–711.
- Guo, S., Wang, J., Xiong, L., Ying, A., Li, D., 2002. A macro-scale and semi-distributed monthly water balance model to predict climate change impacts in China. *Journal of Hydrology* 268 (1), 1–15.
- Hunter, T. S., Clites, A. H., Campbell, K. B., Gronewold, A. D., 2015. Development and application of a North American Great Lakes hydro-meteorological database Part I: Precipitation, evaporation, runoff, and air temperature. *Journal of Great Lakes Research* 41 (1), 65–77.
- Jin, K.-R., Hamrick, J. H., Tisdale, T., 2000. Application of three-dimensional hydrodynamic model for Lake Okeechobee. *Journal of Hydraulic Engineering* 126 (10), 758–771.
- Joseph, J., Guillaume, J. H., 2013. Using a parallelized MCMC algorithm in R to identify appropriate likelihood functions for SWAT. *Environmental Modelling & Software* 46, 292–298.
- Kebede, S., Travi, Y., Alemayehu, T., Marc, V., 2006. Water balance of Lake Tana and its sensitivity to fluctuations in rainfall, Blue Nile basin, Ethiopia. *Journal of Hydrology* 316 (1), 233–247.
- Kim, C., Stricker, J., 1996. Influence of spatially variable soil hydraulic properties and rainfall intensity on the water budget. *Water Resources Research* 32 (6), 1699–1712.
- Kruschke, J. K., 2013. Posterior predictive checks can and should be Bayesian: Comment on Gelman and Shalizi, 'Philosophy and the practice of Bayesian statistics'. *British Journal of Mathematical and Statistical Psychology* 66 (1), 45–56.

- Lespinas, F., Fortin, V., Roy, G., Rasmussen, P., Stadnyk, T., 2015. Performance evaluation of the Canadian Precipitation Analysis (CaPA). *Journal of Hydrometeorology* 16 (5), 2045–2064.
- Li, M., Wang, Q., Bennett, J., 2013. Accounting for seasonal dependence in hydrological model errors and prediction uncertainty. *Water Resources Research* 49 (9), 5913–5929.
- Li, X.-Y., Xu, H.-Y., Sun, Y.-L., Zhang, D.-S., Yang, Z.-P., 2007. Lake-level change and water balance analysis at Lake Qinghai, West China during recent decades. *Water Resources Management* 21 (9), 1505–1516.
- Makhoul, Z., Michel, C., 1994. A two-parameter monthly water balance model for French watersheds. *Journal of Hydrology* 162 (3), 299–318.
- Malve, O., Laine, M., Haario, H., Kirkkala, T., Sarvala, J., 2007. Bayesian modelling of algal mass occurrences using adaptive MCMC methods with a lake water quality model. *Environmental Modelling & Software* 22 (7), 966–977.
- Martine, G., McGranahan, G., Montgomery, M., Fernandez-Castilla, R., 2008. *The New Global Frontier: Urbanization, Poverty, and Environment in the 21st Century*. Routledge Earthscan, New York, NY.
- Milly, P. C., Betancourt, J., Falkenmark, M., Hirsch, R. M., Kundzewicz, Z. W., Lettenmaier, D. P., Stouffer, R. J., 2008. Stationarity is dead: whither water management? *Science* 319 (5863), 573–574.
- Montgomery, D. C., 2008. *Design and Analysis of Experiments*. John Wiley & Sons.
- Mouelhi, S., Michel, C., Perrin, C., Andréassian, V., 2006. Stepwise development of a two-parameter monthly water balance model. *Journal of Hydrology* 318 (1), 200–214.
- Mueller, D. S., Abad, J. D., Garcia, C. M., Gartner, J. W., Garcia, M. H., Oberg, K. A., 2007. Errors in acoustic Doppler profiler velocity measurements caused by flow disturbance. *Journal of Hydraulic Engineering* 133 (12), 1411–1420.

- Pan, M., Wood, E. F., 2006. Data assimilation for estimating the terrestrial water budget using a constrained ensemble Kalman filter. *Journal of Hydrometeorology* 7 (3), 534–547.
- Plummer, M., et al., 2003. JAGS: A program for analysis of Bayesian graphical models using Gibbs sampling. In: Proceedings of the 3rd international workshop on distributed statistical computing. Vol. 124. Vienna, p. 125.
- Quinn, F. H., Guerra, B., 1986. Current perspectives on the Lake Erie water balance. *Journal of Great Lakes Research* 12 (2), 109–116.
- R Core Team, 2014. R: A language and environment for statistical computing. R Foundation for Statistical Computing, Vienna, Austria.
- Raes, D., Geerts, S., Kipkorir, E., Wellens, J., Sahli, A., 2006. Simulation of yield decline as a result of water stress with a robust soil water balance model. *Agricultural Water Management* 81 (3), 335–357.
- Richey, M., 2010. The evolution of Markov chain Monte Carlo methods. *American Mathematical Monthly* 117 (5), 383–413.
- Rodell, M., Famiglietti, J., Chen, J., Seneviratne, S., Viterbo, P., Holl, S., Wilson, C., 2004. Basin scale estimates of evapotranspiration using GRACE and other observations. *Geophysical Research Letters* 31 (20).
- Schoups, G., Vrugt, J. A., 2010. A formal likelihood function for parameter and predictive inference of hydrologic models with correlated, heteroscedastic, and non-gaussian errors. *Water Resources Research* 46 (10).
- Sheffield, J., Ferguson, C. R., Troy, T. J., Wood, E. F., McCabe, M. F., 2009. Closing the terrestrial water budget from satellite remote sensing. *Geophysical Research Letters* 36 (7).
- Smith, J. P., Hunter, T. S., Clites, A. H., Stow, C. A., Slawek, T., Muhr, G. C., Gronewold, A. D., 2016. An expandable web-based platform for visually analyzing basin-scale hydro-climate time series data. *Environmental Modelling & Software* 78, 97–105.
- United States Geological Survey, 2017. National Water Information Service. Available at <https://waterdata.usgs.gov/nwis/inventory> (2017/02/20).

- Voinov, A., Bousquet, F., 2010. Modelling with stakeholders. *Environmental Modelling and Software* 25 (11), 1268–1281.
- Vörösmarty, C. J., Federer, C. A., Schloss, A. L., 1998. Potential evaporation functions compared on US watersheds: Possible implications for global-scale water balance and terrestrial ecosystem modeling. *Journal of Hydrology* 207 (3), 147–169.
- Vörösmarty, C. J., Green, P., Salisbury, J., Lammers, R. B., 2000. Global water resources: vulnerability from climate change and population growth. *science* 289 (5477), 284–288.
- Xu, C.-Y., Singh, V. P., 1998. A review on monthly water balance models for water resources investigations. *Water Resources Management* 12 (1), 20–50.

# Supplementary Material: Development and analysis of a Bayesian water balance model for large lake systems

Joeseph P. Smith<sup>a</sup>, Andrew D. Gronewold<sup>b,c</sup>

<sup>a</sup>*Cooperative Institute for Great Lakes Research, University of Michigan, Ann Arbor, Michigan USA, 48109*

<sup>b</sup>*Great Lakes Environmental Research Laboratory, National Oceanic and Atmospheric Administration, Ann Arbor, Michigan, USA, 48108*

<sup>c</sup>*Department of Civil and Environmental Engineering, University of Michigan, Ann Arbor, Michigan USA, 48109*

---

---

## 1. Contents

- Page 3 - Prior distributions for Lake Superior's water balance components
- Page 4 - Prior distributions for Lake Michigan-Huron's water balance components
- Page 5 - Prototype model posterior inferences for Lake Superior's water balance components
- Page 6 - Prototype model posterior inferences for Lake Michigan-Huron's water balance components
- Page 7 - f12NF model posterior inferences for Lake Superior's water balance components
- Page 8 - f12NF model posterior inferences for Lake Michigan-Huron's water balance components
- Page 9 - f12FF model posterior inferences for Lake Superior's water balance components

---

\*Corresponding author. Tel.: +1-734-741-2252, Fax: +1 734-741-2055  
Email address: [joeseph@umich.edu](mailto:joeseph@umich.edu) (Joeseph P. Smith)

- Page 10 - f12FF model posterior inferences for Lake Michigan-Huron's water balance components
- Pages 12-17: (f)XXFF model BUGS code
- Pages 18-24: (f)XXHH model BUGS code

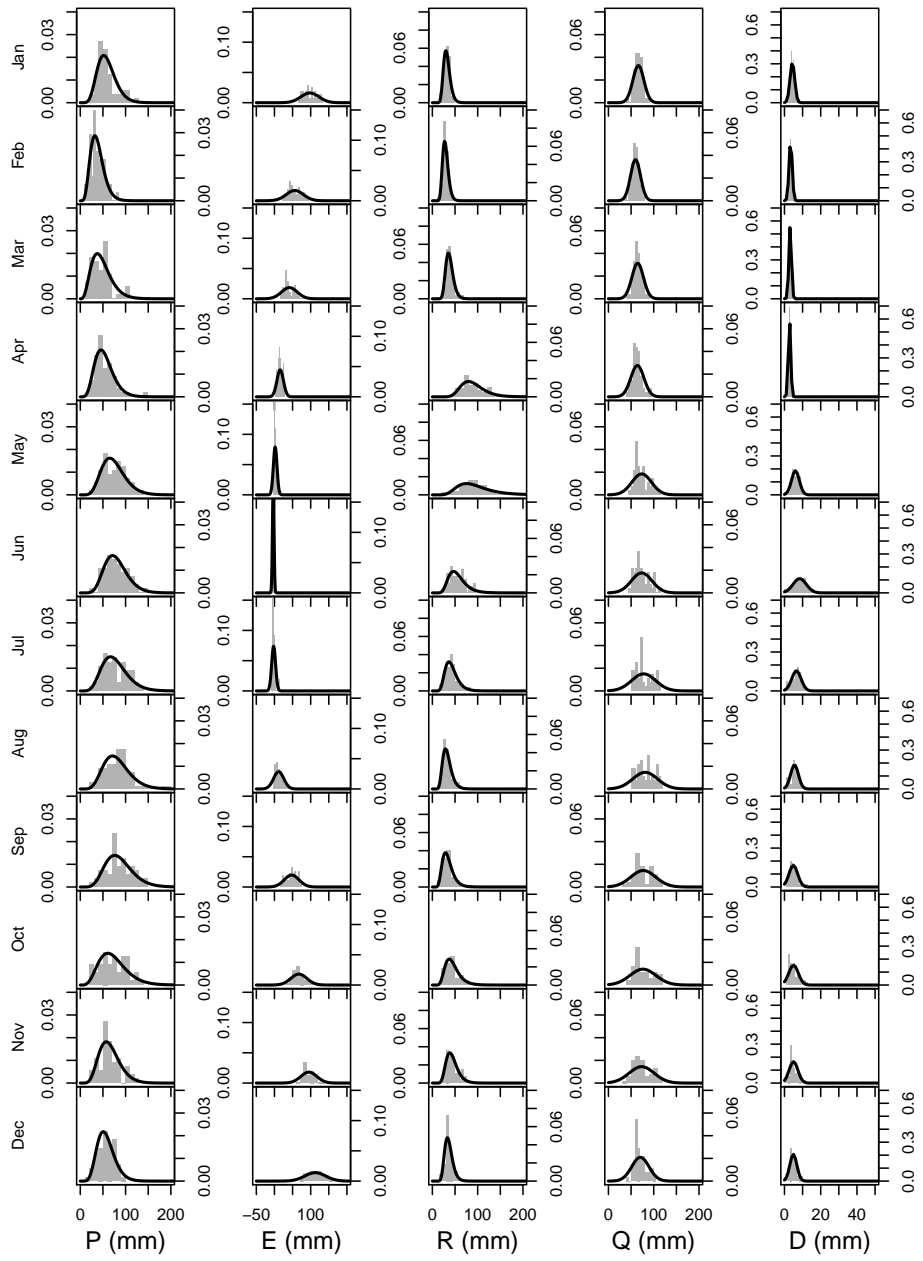


Figure 1: Prior distributions as described in section 2.2.2 for the water water balance components on Lake Superior. Unbordered gray rectangles in the background are histograms of the historical record (1950-2004) from the NOAA-GLERL GLM-HMD and coordinated estimates. Solid lines represent our informative prior distributions.

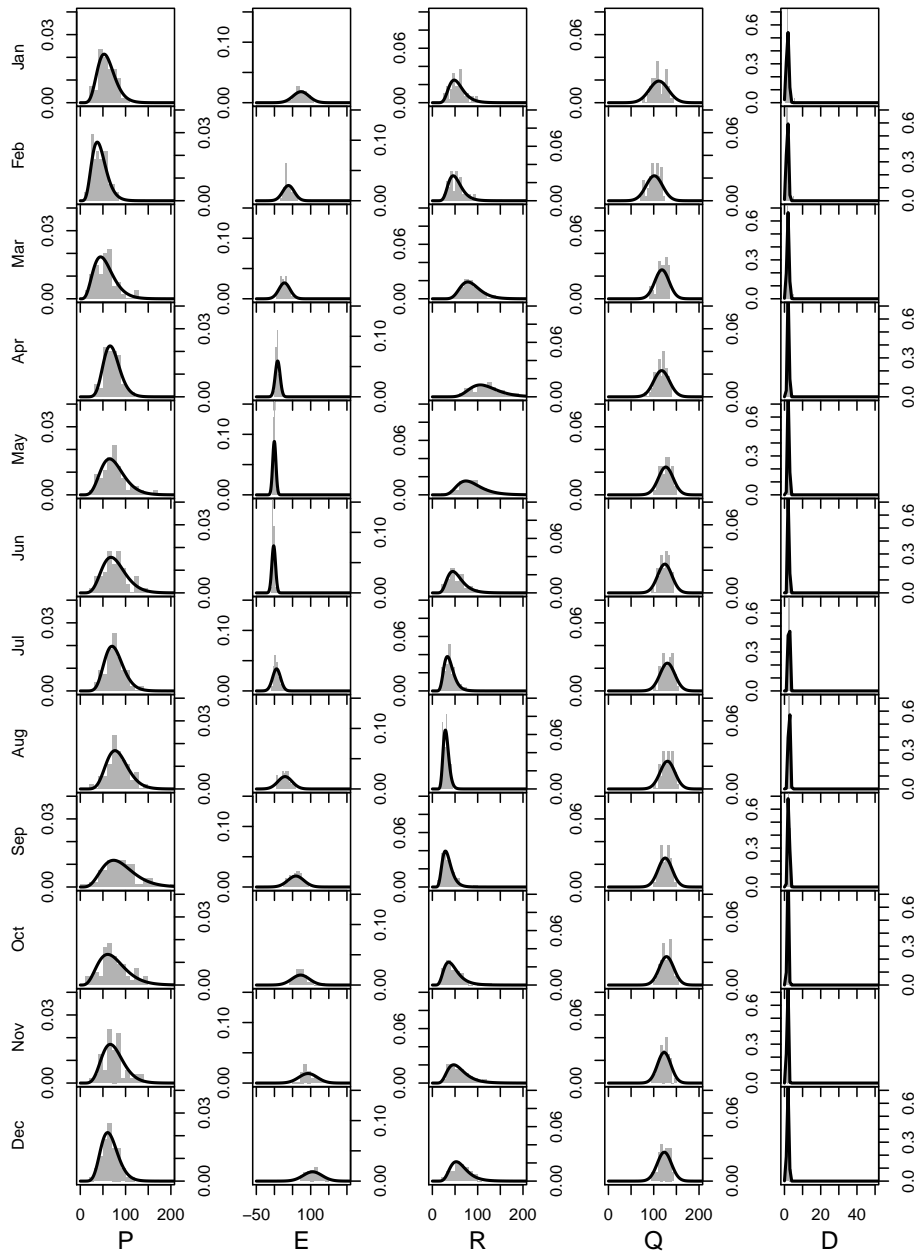


Figure 2: Prior distributions as described in section 2.2.2 for the water water balance components on Lake Michigan-Huron. Unbordered gray rectangles in the background are histograms of the historical record (1950-2004) from the NOAA-GLERL GLM-HMD and coordinated estimates. Solid lines represent our informative prior distributions.

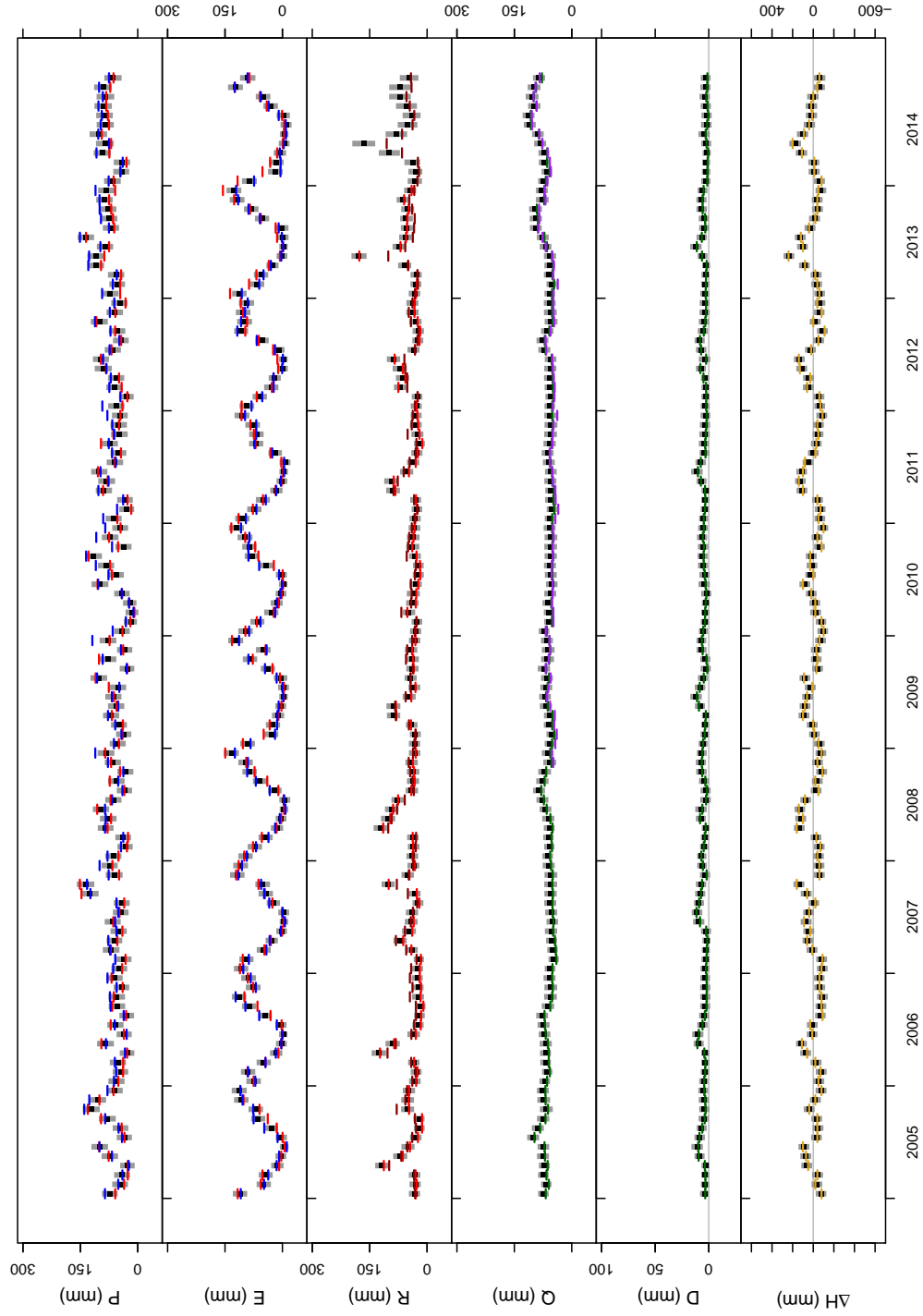


Figure 3: Posterior inferences (gray bars indicate 95% credible intervals, with black squares for the median estimates) from the prototype model for Lake Superior's water water balance components. For P and E, the red segments represent data from the NOAA-GLERL GLM-HMD, and the blue segments from GEM-MESH. For R, red segments also represent the GLM-HMD, and the darker red segments represent the NOAA-GLERL LBRM. For Q and D, the green segments are coordinated estimates, purple segments for international gauging stations. For  $\Delta H$ , the gold segments represent coordinated estimates of month-to-month change in storage, or  $y_{\Delta H, t, 1}$  while gray bars represent the posterior predictive distributions for those estimates.

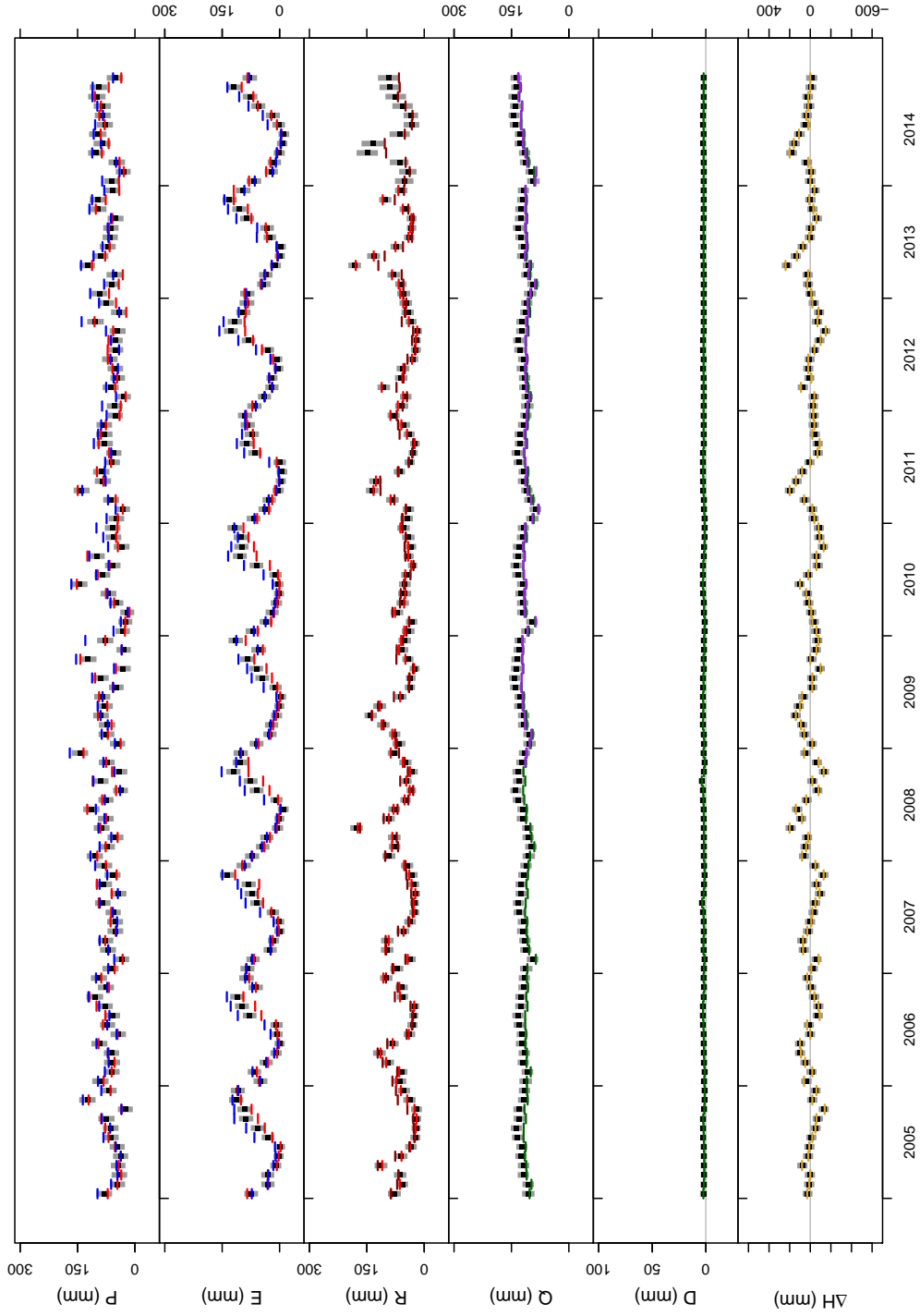


Figure 4: Posterior inferences (gray bars indicate 95% credible intervals, with black squares for the median estimates) from the prototype model for Lake Michigan-Huron's water water balance components. For P and E, the red segments represent data from the NOAA-GLERL GLM-HMD, and the blue segments from GEM-MESH. For R, red segments also represent the GLM-HMD, and the darker red segments represent the NOAA-GLERL LBRM. For Q and D, the green segments are coordinated estimates, purple segments for international gauging stations. For  $\Delta H$ , the gold segments represent coordinated estimates of month-to-month change in storage, or  $y_{\Delta H, t, 1}$  while gray bars represent the posterior predictive distributions for those estimates.

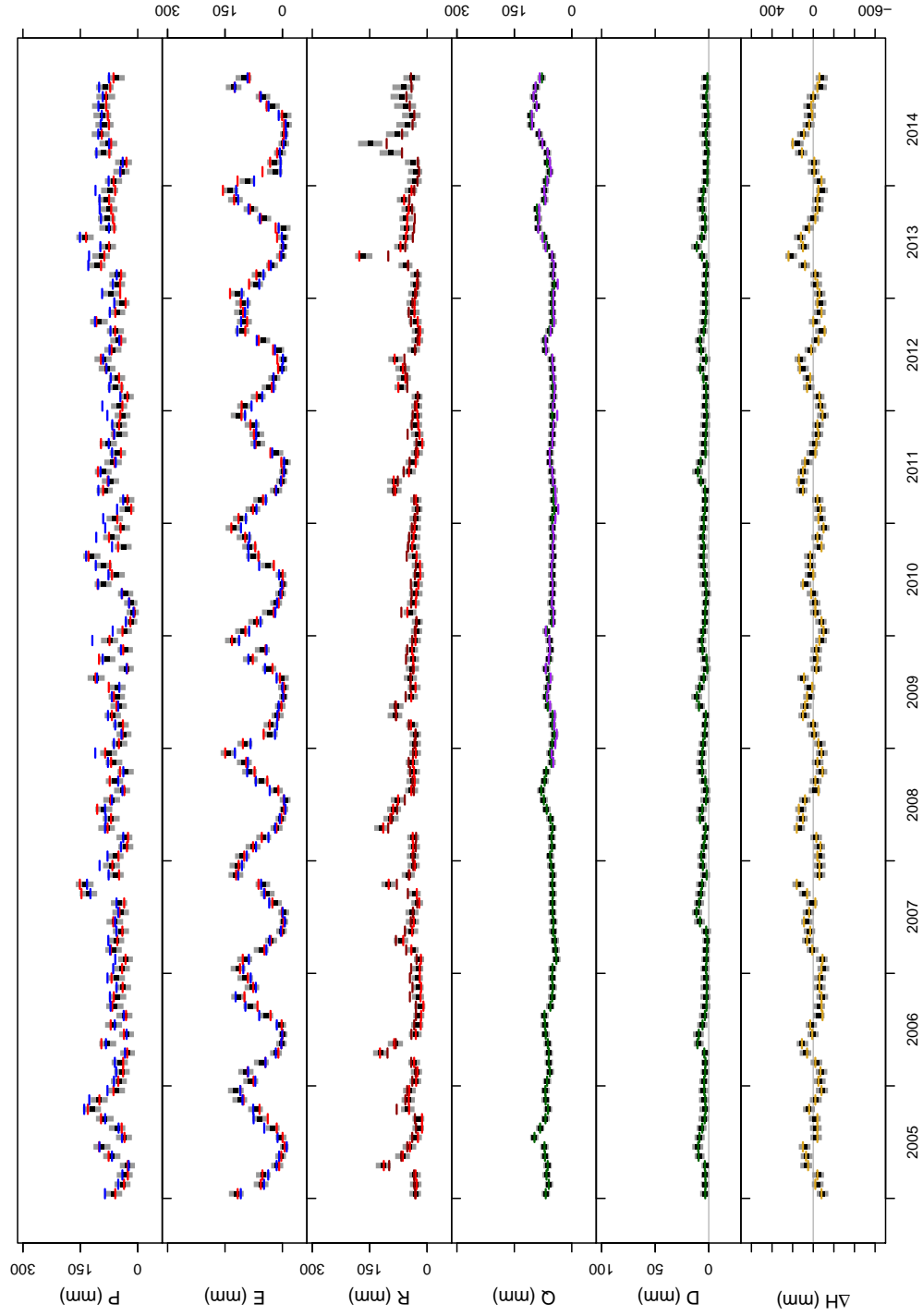


Figure 5: Posterior inferences (gray bars indicate 95% credible intervals, with black squares for the median estimates) from the f12NF model for Lake Superior's water water balance components. For P and E, the red segments represent data from the NOAA-GLERL GLM-HMD, and the blue segments from GEM-MESH. For R, red segments also represent the GLM-HMD, and the darker red segments represent the NOAA-GLERL LBRM. For Q and D, the green segments are coordinated estimates, purple segments for international gauging stations. For  $\Delta H$ , the gold segments represent coordinated estimates of month-to-month change in storage, or  $y_{\Delta H, t, 1}$  while gray bars represent the posterior predictive distributions for those estimates.

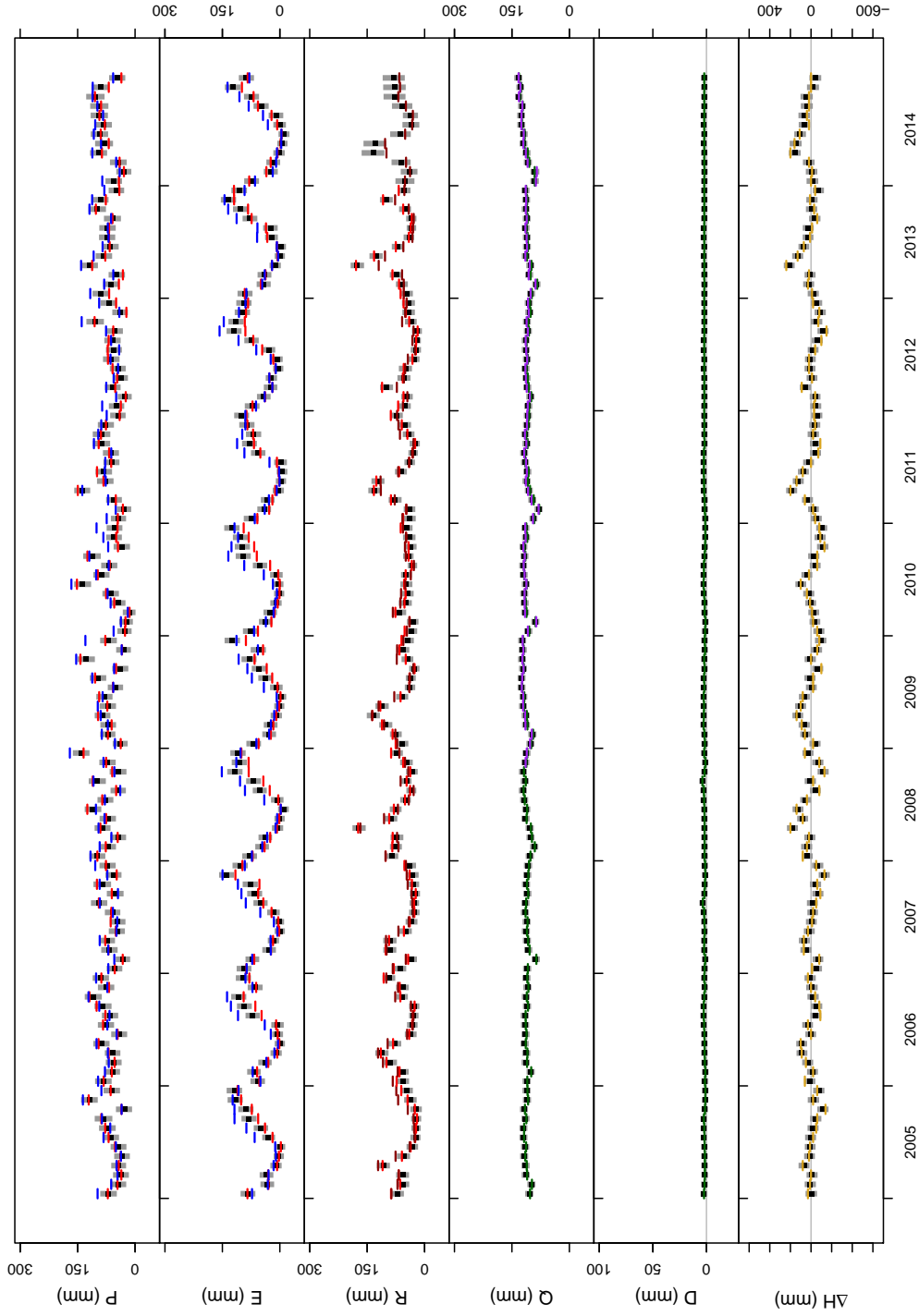


Figure 6: Posterior inferences (gray bars indicate 95% credible intervals, with black squares for the median estimates) from the f12NF model for Lake Michigan-Huron's water water balance components. For P and E, the red segments represent data from the NOAA-GLERL GLM-HMD, and the blue segments from GEM-MESH. For R, red segments also represent the GLM-HMD, and the darker red segments represent the NOAA-GLERL LBRM. For Q and D, the green segments are coordinated estimates, purple segments for international gauging stations. For  $\Delta H$ , the gold segments represent coordinated estimates of month-to-month change in storage, or  $y_{\Delta H, t, 1}$  while gray bars represent the posterior predictive distributions for those estimates.

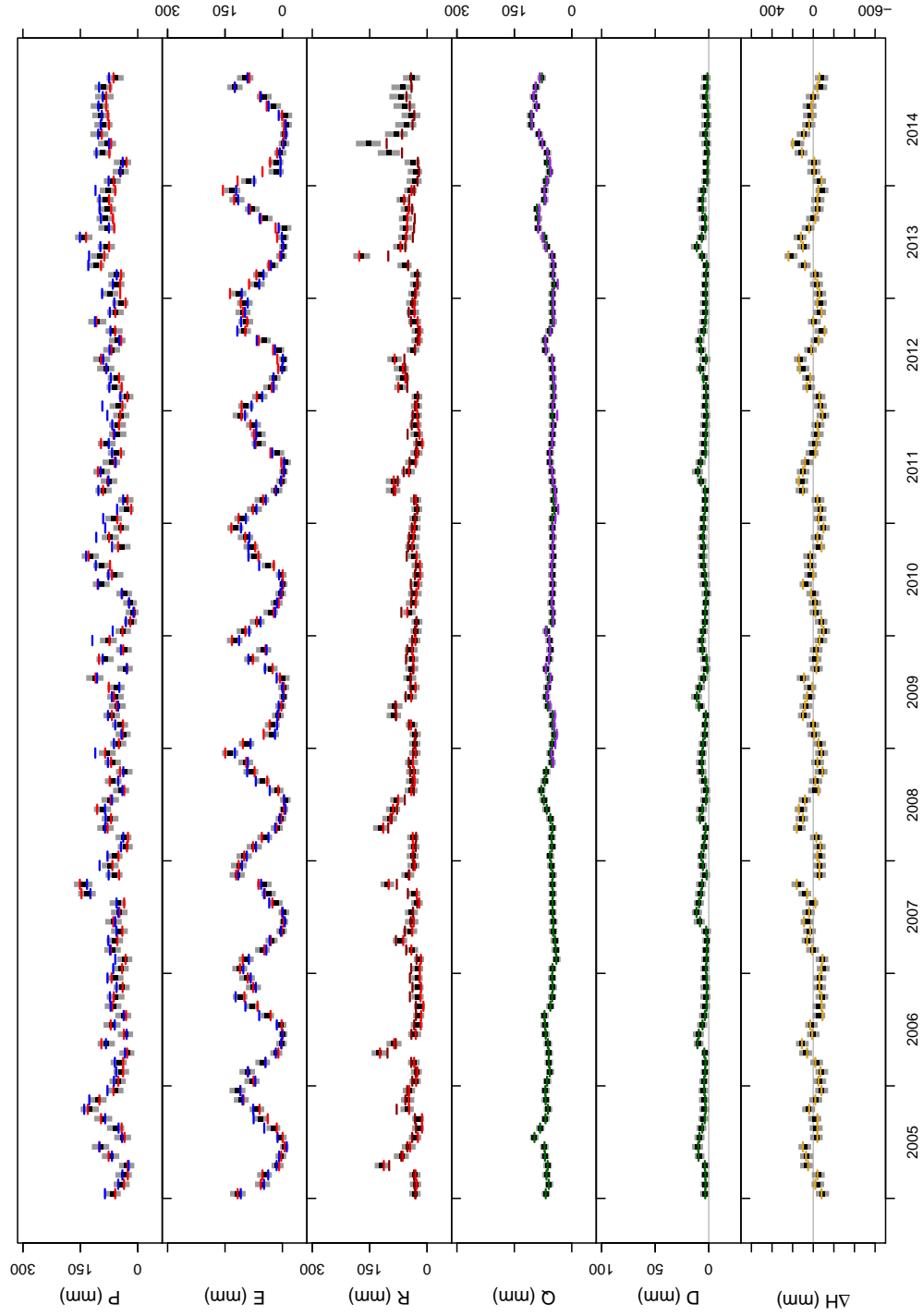


Figure 7: Posterior inferences (gray bars indicate 95% credible intervals, with black squares for the median estimates) from the f12FF model for Lake Superior’s water water balance components. For P and E, the red segments represent data from the NOAA-GLERL GLM-HMD, and the blue segments from GEM-MESH. For R, red segments also represent the GLM-HMD, and the darker red segments represent the NOAA-GLERL LBRM. For Q and D, the green segments are coordinated estimates, purple segments for international gauging stations. For  $\Delta H$ , the gold segments represent coordinated estimates of month-to-month change in storage, or  $y_{\Delta H, t, 1}$  while gray bars represent the posterior predictive distributions for those estimates.

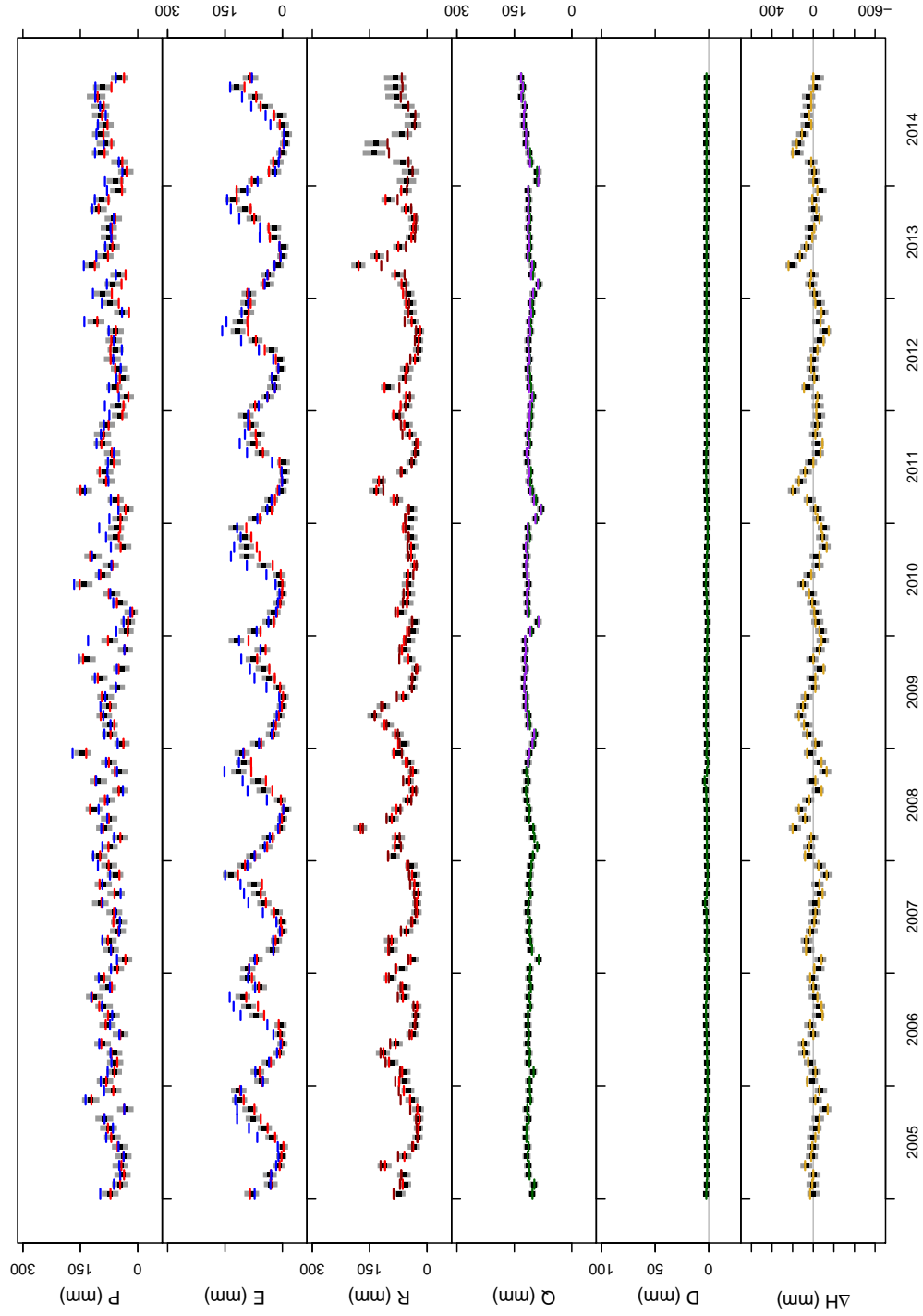


Figure 8: Posterior inferences (gray bars indicate 95% credible intervals, with black squares for the median estimates) from the f12FF model for Lake Michigan-Huron's water water balance components. For P and E, the red segments represent data from the NOAA-GLERL GLM-HMD, and the blue segments from GEM-MESH. For R, red segments also represent the GLM-HMD, and the darker red segments represent the NOAA-GLERL LBRM. For Q and D, the green segments are coordinated estimates, purple segments for international gauging stations. For  $\Delta H$ , the gold segments represent coordinated estimates of month-to-month change in storage, or  $y_{\Delta H, t, 1}$  while gray bars represent the posterior predictive distributions for those estimates.

MODEL CODE

```

## (f) 12FF MODEL WITH POSTERIOR PREDICTIVE DISTRIBUTIONS FOR ALL VARIABLES

model {
  for (j in posteriorStartMonth:posteriorEndMonth) {

    ##### Priors as described in section 2.2.2
    ## Data are fed in through R in jags.model
    ## function call, via data parameter
    ## Note: distribution parameters are
    ## mean and precision
    ## precision = 1/variance
    #####
    #### SUPERIOR
    superiorPrecip[j] ~ dgamma(superiorPriorPrecipShape[m[j]], superiorPriorPrecipRate[m[j]])
    superiorEvap[j] ~ dnorm(superiorEvapPriorMean[m[j]], superiorEvapPriorPrecision[m[j]])
    superiorRunoff[j] <- exp(superiorLogRunoff[j])
    superiorLogRunoff[j] ~ dnorm(superiorRunoffLogPriorMean[m[j]], superiorRunoffLogPriorPrecision[m[j]])
    superiorOutflow[j] ~ dnorm(superiorOutflowPriorMean[m[j]], superiorOutflowPriorPrecision[m[j]])
    superiorDiversion[j] ~ dnorm(superiorDiversionPriorMean[m[j]], superiorDiversionPriorPrecision[m[j]])

    #### MICHIGAN-HURON
    miHuronPrecip[j] ~ dgamma(miHuronPriorPrecipShape[m[j]], miHuronPriorPrecipRate[m[j]])
    miHuronEvap[j] ~ dnorm(miHuronEvapPriorMean[m[j]], miHuronEvapPriorPrecision[m[j]])
    miHuronRunoff[j] <- exp(miHuronLogRunoff[j])
    miHuronLogRunoff[j] ~ dnorm(miHuronRunoffLogPriorMean[m[j]], miHuronRunoffLogPriorPrecision[m[j]])
    miHuronOutflow[j] ~ dnorm(miHuronOutflowPriorMean[m[j]], miHuronOutflowPriorPrecision[m[j]])
    miHuronDiversion[j] ~ dnorm(miHuronDiversionPriorMean[m[j]], miHuronDiversionPriorPrecision[m[j]])

    #####
    ## Likelihood functions as described in section 2.2.2
    ## Biases follow equation 6
    #####
    #### SUPERIOR
    ySuperiorPrecip1[j] ~ dnorm(ySuperiorPrecip1Mean[j], ySuperiorPrecip1Prec)
    ySuperiorPrecip2[j] ~ dnorm(ySuperiorPrecip2Mean[j], ySuperiorPrecip2Prec)
    ySuperiorEvap1[j] ~ dnorm(ySuperiorEvap1Mean[j], ySuperiorEvap1Prec)
    ySuperiorEvap2[j] ~ dnorm(ySuperiorEvap2Mean[j], ySuperiorEvap2Prec)
    ySuperiorRunoff1[j] ~ dnorm(ySuperiorRunoff1Mean[j], ySuperiorRunoff1Prec)
    ySuperiorRunoff2[j] ~ dnorm(ySuperiorRunoff2Mean[j], ySuperiorRunoff2Prec)
    ySuperiorOutflow1[j] ~ dnorm(ySuperiorOutflow1Mean[j], ySuperiorOutflow1Prec)
    ySuperiorOutflow2[j] ~ dnorm(ySuperiorOutflow2Mean[j], ySuperiorOutflow2Prec)
    ySuperiorDiversion1[j] ~ dnorm(ySuperiorDiversion1Mean[j], ySuperiorDiversion1Prec)

    ySuperiorPrecip1Mean[j] <- superiorPrecip[j] + ySuperiorPrecip1Bias[m[j]]
    ySuperiorPrecip2Mean[j] <- superiorPrecip[j] + ySuperiorPrecip2Bias[m[j]]
    ySuperiorEvap1Mean[j] <- superiorEvap[j] + ySuperiorEvap1Bias[m[j]]
    ySuperiorEvap2Mean[j] <- superiorEvap[j] + ySuperiorEvap2Bias[m[j]]
    ySuperiorRunoff1Mean[j] <- superiorRunoff[j] + ySuperiorRunoff1Bias[m[j]]
    ySuperiorRunoff2Mean[j] <- superiorRunoff[j] + ySuperiorRunoff2Bias[m[j]]
    ySuperiorOutflow1Mean[j] <- superiorOutflow[j] + ySuperiorOutflow1Bias[m[j]]
    ySuperiorOutflow2Mean[j] <- superiorOutflow[j] + ySuperiorOutflow2Bias[m[j]]
    ySuperiorDiversion1Mean[j] <- superiorDiversion[j] + ySuperiorDiversion1Bias[m[j]]
  }
}

```

```

#### MICHIGAN-HURON
yMiHuronPrecip1[j] ~ dnorm(yMiHuronPrecip1Mean[j], yMiHuronPrecip1Prec)
yMiHuronPrecip2[j] ~ dnorm(yMiHuronPrecip2Mean[j], yMiHuronPrecip2Prec)
yMiHuronEvap1[j] ~ dnorm(yMiHuronEvap1Mean[j], yMiHuronEvap1Prec)
yMiHuronEvap2[j] ~ dnorm(yMiHuronEvap2Mean[j], yMiHuronEvap2Prec)
yMiHuronRunoff1[j] ~ dnorm(yMiHuronRunoff1Mean[j], yMiHuronRunoff1Prec)
yMiHuronRunoff2[j] ~ dnorm(yMiHuronRunoff2Mean[j], yMiHuronRunoff2Prec)
yMiHuronOutflow1[j] ~ dnorm(yMiHuronOutflow1Mean[j], yMiHuronOutflow1Prec)
yMiHuronOutflow2[j] ~ dnorm(yMiHuronOutflow2Mean[j], yMiHuronOutflow2Prec)
yMiHuronDiversion1[j] ~ dnorm(yMiHuronDiversion1Mean[j], yMiHuronDiversion1Prec)

yMiHuronPrecip1Mean[j] <- miHuronPrecip[j] + yMiHuronPrecip1Bias[m[j]]
yMiHuronPrecip2Mean[j] <- miHuronPrecip[j] + yMiHuronPrecip2Bias[m[j]]
yMiHuronEvap1Mean[j] <- miHuronEvap[j] + yMiHuronEvap1Bias[m[j]]
yMiHuronEvap2Mean[j] <- miHuronEvap[j] + yMiHuronEvap2Bias[m[j]]
yMiHuronRunoff1Mean[j] <- miHuronRunoff[j] + yMiHuronRunoff1Bias[m[j]]
yMiHuronRunoff2Mean[j] <- miHuronRunoff[j] + yMiHuronRunoff2Bias[m[j]]
yMiHuronOutflow1Mean[j] <- miHuronOutflow[j] + yMiHuronOutflow1Bias[m[j]]
yMiHuronOutflow2Mean[j] <- miHuronOutflow[j] + yMiHuronOutflow2Bias[m[j]]
yMiHuronDiversion1Mean[j] <- miHuronDiversion[j] + yMiHuronDiversion1Bias[m[j]]


}

#####
# Water balance model as described in section 2.1
# Model/Process error follows equation 4
#####

for(k in rollPeriod:posteriorEndMonth){
  ### SUPERIOR
  ySuperiorRStore[k] ~ dnorm(superiorRStore[k], ySuperiorRStorePrec)

  superiorRStore[k] <- (
    sum(superiorPrecip[(k-rollPeriod+1):k])
    -sum(superiorEvap[(k-rollPeriod+1):k])
    +sum(superiorRunoff[(k-rollPeriod+1):k])
    -sum(superiorOutflow[(k-rollPeriod+1):k])
    +sum(superiorDiversion[(k-rollPeriod+1):k])
    +sum(superiorProcError[m[(k-rollPeriod+1):k]])
  )

  ### MICHIGAN-HURON
  yMiHuronRStore[k] ~ dnorm(miHuronRStore[k], yMiHuronRStorePrec)

  miHuronRStore[k] <- (
    sum(miHuronPrecip[(k-rollPeriod+1):k])
    -sum(miHuronEvap[(k-rollPeriod+1):k])
    +sum(miHuronRunoff[(k-rollPeriod+1):k])
    -sum(miHuronOutflow[(k-rollPeriod+1):k])
    +0.70110653739*sum(superiorOutflow[(k-rollPeriod+1):k])
    -sum(miHuronDiversion[(k-rollPeriod+1):k])
  )
}

```

```

        +sum(miHuronProcError[m[(k-rollPeriod+1):k]])
    )
}

#####
## Bias terms and process errors, equations 4 and 6 respectively
## Includes incorporation of expert guidance on Q and D
## They would otherwise have the same bias definition as the other
## variables
#####
for (i in 1:12){
  ySuperiorPrecip1Bias[i] ~ dnorm(0,0.01)
  ySuperiorPrecip2Bias[i] ~ dnorm(0,0.01)
  ySuperiorEvap1Bias[i] ~ dnorm(0,0.01)
  ySuperiorEvap2Bias[i] ~ dnorm(0,0.01)
  ySuperiorRunoff1Bias[i] ~ dnorm(0,0.01)
  ySuperiorRunoff2Bias[i] ~ dnorm(0,0.01)
  ySuperiorOutflow1Bias[i] ~ dnorm(0,0.25)
  ySuperiorOutflow2Bias[i] ~ dnorm(0,0.25)
  ySuperiorDiversion1Bias[i] ~ dnorm(0,0.25)

  yMiHuronPrecip1Bias[i] ~ dnorm(0,0.01)
  yMiHuronPrecip2Bias[i] ~ dnorm(0,0.01)
  yMiHuronEvap1Bias[i] ~ dnorm(0,0.01)
  yMiHuronEvap2Bias[i] ~ dnorm(0,0.01)
  yMiHuronRunoff1Bias[i] ~ dnorm(0,0.01)
  yMiHuronRunoff2Bias[i] ~ dnorm(0,0.01)
  yMiHuronOutflow1Bias[i] ~ dnorm(0,0.25)
  yMiHuronOutflow2Bias[i] ~ dnorm(0,0.25)
  yMiHuronDiversion1Bias[i] ~ dnorm(0,0.25)

  superiorProcError[i] ~ dnorm(0,0.01)
  miHuronProcError[i] ~ dnorm(0,0.01)
}

#####
## Precision for Observations
#####

### SUPERIOR
ySuperiorRStorePrec ~ dgamma(0.01,0.01)
ySuperiorPrecip1Prec ~ dgamma(0.1,0.1)
ySuperiorPrecip2Prec ~ dgamma(0.1,0.1)
ySuperiorEvap1Prec ~ dgamma(0.1,0.1)
ySuperiorEvap2Prec ~ dgamma(0.1,0.1)
ySuperiorRunoff1Prec ~ dgamma(0.1,0.1)
ySuperiorRunoff2Prec ~ dgamma(0.1,0.1)
ySuperiorOutflow1Prec ~ dgamma(0.1,0.1)
ySuperiorOutflow2Prec ~ dgamma(0.1,0.1)
ySuperiorDiversion1Prec ~ dgamma(0.1,0.1)

### MICHIGAN-HURON
yMiHuronRStorePrec ~ dgamma(0.01,0.01)
yMiHuronPrecip1Prec ~ dgamma(0.1,0.1)
yMiHuronPrecip2Prec ~ dgamma(0.1,0.1)
yMiHuronEvap1Prec ~ dgamma(0.1,0.1)
yMiHuronEvap2Prec ~ dgamma(0.1,0.1)

```

```

yMiHuronRunoff1Prec ~ dgamma(0.1,0.1)
yMiHuronRunoff2Prec ~ dgamma(0.1,0.1)
yMiHuronOutflow1Prec ~ dgamma(0.1,0.1)
yMiHuronOutflow2Prec ~ dgamma(0.1,0.1)
yMiHuronDiversion1Prec ~ dgamma(0.1,0.1)

#####
# Posterior predictive (PP) distributions for verification
#####

for(jp in posteriorStartMonth:posteriorEndMonth) {
  ### SUPERIOR
  ySuperiorPrecip1PP[jp] ~ dnorm(ySuperiorPrecip1Mean[jp], ySuperiorPrecip1Prec)
  ySuperiorPrecip2PP[jp] ~ dnorm(ySuperiorPrecip2Mean[jp], ySuperiorPrecip2Prec)
  ySuperiorEvap1PP[jp] ~ dnorm(ySuperiorEvap1Mean[jp], ySuperiorEvap1Prec)
  ySuperiorEvap2PP[jp] ~ dnorm(ySuperiorEvap2Mean[jp], ySuperiorEvap2Prec)
  ySuperiorRunoff1PP[jp] ~ dnorm(ySuperiorRunoff1Mean[jp], ySuperiorRunoff1Prec)
  ySuperiorRunoff2PP[jp] ~ dnorm(ySuperiorRunoff2Mean[jp], ySuperiorRunoff2Prec)
  ySuperiorOutflow1PP[jp] ~ dnorm(ySuperiorOutflow1Mean[jp], ySuperiorOutflow1Prec)
  ySuperiorOutflow2PP[jp] ~ dnorm(ySuperiorOutflow2Mean[jp], ySuperiorOutflow2Prec)
  ySuperiorDiversion1PP[jp] ~ dnorm(ySuperiorDiversion1Mean[jp], ySuperiorDiversion1Prec)

  ### MICHIGAN-HURON
  yMiHuronPrecip1PP[jp] ~ dnorm(yMiHuronPrecip1Mean[jp], yMiHuronPrecip1Prec)
  yMiHuronPrecip2PP[jp] ~ dnorm(yMiHuronPrecip2Mean[jp], yMiHuronPrecip2Prec)
  yMiHuronEvap1PP[jp] ~ dnorm(yMiHuronEvap1Mean[jp], yMiHuronEvap1Prec)
  yMiHuronEvap2PP[jp] ~ dnorm(yMiHuronEvap2Mean[jp], yMiHuronEvap2Prec)
  yMiHuronRunoff1PP[jp] ~ dnorm(yMiHuronRunoff1Mean[jp], yMiHuronRunoff1Prec)
  yMiHuronRunoff2PP[jp] ~ dnorm(yMiHuronRunoff2Mean[jp], yMiHuronRunoff2Prec)
  yMiHuronOutflow1PP[jp] ~ dnorm(yMiHuronOutflow1Mean[jp], yMiHuronOutflow1Prec)
  yMiHuronOutflow2PP[jp] ~ dnorm(yMiHuronOutflow2Mean[jp], yMiHuronOutflow2Prec)
  yMiHuronDiversion1PP[jp] ~ dnorm(yMiHuronDiversion1Mean[jp], yMiHuronDiversion1Prec)

  # MONTH BY MONTH CHANGE IN STORAGE ANALYSIS

  ySuperiorDStorePP[jp] ~ dnorm(superiorDStore[jp], ySuperiorRStorePrec)

  superiorDStore[jp] <- (
    superiorPrecip[jp]
    -superiorEvap[jp]
    +superiorRunoff[jp]
    -superiorOutflow[jp]
    +superiorDiversion[jp]
    +superiorProcError[m[jp]]
  )

  yMiHuronDStorePP[jp] ~ dnorm(miHuronDStore[jp], yMiHuronRStorePrec)

  miHuronDStore[jp] <- (
    miHuronPrecip[jp]
    -miHuronEvap[jp]
    +miHuronRunoff[jp]
    +0.70110653739*superiorOutflow[jp]
  )
}

```

```

        -miHuronOutflow[jp]
        -miHuronDiversion[jp]
        +miHuronProcError[m[jp]]
    )
}

### ROLLING SUM STORAGE ANALYSIS

# 1 YEAR

for(x in 12:posteriorEndMonth){
  ySuperiorR1YStorePP[x] ~ dnorm(superiorR1YStore[x], ySuperiorRStorePrec)

  superiorR1YStore[x] <- (
    sum(superiorPrecip[(x-12+1):x])
    -sum(superiorEvap[(x-12+1):x])
    +sum(superiorRunoff[(x-12+1):x])
    -sum(superiorOutflow[(x-12+1):x])
    +sum(superiorDiversion[(x-12+1):x])
    +sum(superiorProcError[m[(x-12+1):x]])
  )

  yMiHuronR1YStorePP[x] ~ dnorm(miHuronR1YStore[x], yMiHuronRStorePrec)

  miHuronR1YStore[x] <- (
    sum(miHuronPrecip[(x-12+1):x])
    -sum(miHuronEvap[(x-12+1):x])
    +sum(miHuronRunoff[(x-12+1):x])
    +0.70110653739*sum(superiorOutflow[(x-12+1):x])
    -sum(miHuronOutflow[(x-12+1):x])
    -sum(miHuronDiversion[(x-12+1):x])
    +sum(miHuronProcError[m[(x-12+1):x]])
  )
}

# 5 YEAR

for(z in 60:posteriorEndMonth){
  ySuperiorR5YStorePP[z] ~ dnorm(superiorR5YStore[z], ySuperiorRStorePrec)

  superiorR5YStore[z] <- (
    sum(superiorPrecip[(z-60+1):z])
    -sum(superiorEvap[(z-60+1):z])
    +sum(superiorRunoff[(z-60+1):z])
    -sum(superiorOutflow[(z-60+1):z])
    +sum(superiorDiversion[(z-60+1):z])
    +sum(superiorProcError[m[(z-60+1):z]])
  )

  yMiHuronR5YStorePP[z] ~ dnorm(miHuronR5YStore[z], yMiHuronRStorePrec)

  miHuronR5YStore[z] <- (
    sum(miHuronPrecip[(z-60+1):z])
    -sum(miHuronEvap[(z-60+1):z])
    +sum(miHuronRunoff[(z-60+1):z])
  )
}

```

```
+0.70110653739*sum(superiorOutflow[(z-60+1):z])
-sum(miHuronOutflow[(z-60+1):z])
-sum(miHuronDiversion[(z-60+1):z])
+sum(miHuronProcError[m[(z-60+1):z]])
)
}
}

# END MODEL
```

```

##### (f) 12HH MODEL WITH POSTERIOR PREDICTIVE DISTRIBUTIONS FOR ALL VARIABLES

model {
  for (j in posteriorStartMonth:posteriorEndMonth){

    ##########
    ## Priors as described in section 2.2.2
    ## Model/Process errors follow equation set 5
    ## Data are fed in through R in jags.model
    ## function call, via data parameter
    ## Note: distribution parameters are
    ## mean and precision
    ## precision = 1/variance
    ##########

    ##### SUPERIOR
    superiorPrecip[j] ~ dgamma(superiorPriorPrecipShape[m[j]], superiorPriorPrecipRate[m[j]])
    superiorEvap[j] ~ dnorm(superiorEvapPriorMean[m[j]], superiorEvapPriorPrecision[m[j]])
    superiorRunoff[j] <- exp(superiorLogRunoff[j])
    superiorLogRunoff[j] ~ dnorm(superiorRunoffLogPriorMean[m[j]], superiorRunoffLogPriorPrecision[m[j]])
    superiorOutflow[j] ~ dnorm(superiorOutflowPriorMean[m[j]], superiorOutflowPriorPrecision[m[j]])
    superiorDiversion[j] ~ dnorm(superiorDiversionPriorMean[m[j]], superiorDiversionPriorPrecision[m[j]])
    superiorProcError_i[j] ~ dnorm(superiorProcError[m[j]], superiorProcError_iPrec[m[j]])

    ##### MICHIGAN-HURON
    miHuronPrecip[j] ~ dgamma(miHuronPriorPrecipShape[m[j]], miHuronPriorPrecipRate[m[j]])
    miHuronEvap[j] ~ dnorm(miHuronEvapPriorMean[m[j]], miHuronEvapPriorPrecision[m[j]])
    miHuronRunoff[j] <- exp(miHuronLogRunoff[j])
    miHuronLogRunoff[j] ~ dnorm(miHuronRunoffLogPriorMean[m[j]], miHuronRunoffLogPriorPrecision[m[j]])
    miHuronOutflow[j] ~ dnorm(miHuronOutflowPriorMean[m[j]], miHuronOutflowPriorPrecision[m[j]])
    miHuronDiversion[j] ~ dnorm(miHuronDiversionPriorMean[m[j]], miHuronDiversionPriorPrecision[m[j]])
    miHuronProcError_i[j] ~ dnorm(miHuronProcError[m[j]], miHuronProcError_iPrec[m[j]])

    ##########
    ## Likelihood functions as described in section 2.2.2
    ## Biases follow equation set 7
    ##########

    ##### SUPERIOR
    ySuperiorPrecip1[j] ~ dnorm(ySuperiorPrecip1Mean[j], ySuperiorPrecip1Prec)
    ySuperiorPrecip2[j] ~ dnorm(ySuperiorPrecip2Mean[j], ySuperiorPrecip2Prec)
    ySuperiorEvap1[j] ~ dnorm(ySuperiorEvap1Mean[j], ySuperiorEvap1Prec)
    ySuperiorEvap2[j] ~ dnorm(ySuperiorEvap2Mean[j], ySuperiorEvap2Prec)
    ySuperiorRunoff1[j] ~ dnorm(ySuperiorRunoff1Mean[j], ySuperiorRunoff1Prec)
    ySuperiorRunoff2[j] ~ dnorm(ySuperiorRunoff2Mean[j], ySuperiorRunoff2Prec)
    ySuperiorOutflow1[j] ~ dnorm(ySuperiorOutflow1Mean[j], ySuperiorOutflow1Prec)
    ySuperiorOutflow2[j] ~ dnorm(ySuperiorOutflow2Mean[j], ySuperiorOutflow2Prec)
    ySuperiorDiversion1[j] ~ dnorm(ySuperiorDiversion1Mean[j], ySuperiorDiversion1Prec)

    ySuperiorPrecip1Mean[j] <- superiorPrecip[j] + ySuperiorPrecip1Bias_i[j]
    ySuperiorPrecip2Mean[j] <- superiorPrecip[j] + ySuperiorPrecip2Bias_i[j]
    ySuperiorEvap1Mean[j] <- superiorEvap[j] + ySuperiorEvap1Bias_i[j]
    ySuperiorEvap2Mean[j] <- superiorEvap[j] + ySuperiorEvap2Bias_i[j]
    ySuperiorRunoff1Mean[j] <- superiorRunoff[j] + ySuperiorRunoff1Bias_i[j]
    ySuperiorRunoff2Mean[j] <- superiorRunoff[j] + ySuperiorRunoff2Bias_i[j]
    ySuperiorOutflow1Mean[j] <- superiorOutflow[j] + ySuperiorOutflow1Bias_i[j]
    ySuperiorOutflow2Mean[j] <- superiorOutflow[j] + ySuperiorOutflow2Bias_i[j]
    ySuperiorDiversion1Mean[j] <- superiorDiversion[j] + ySuperiorDiversion1Bias_i[j]
  }
}

```

```

ySuperiorPrecip1Bias_i[j] ~ dnorm(ySuperiorPrecip1Bias[m[j]], ySuperiorPrecip1Bias_iPrec[m[j]]);
ySuperiorPrecip2Bias_i[j] ~ dnorm(ySuperiorPrecip2Bias[m[j]], ySuperiorPrecip2Bias_iPrec[m[j]]);
ySuperiorEvap1Bias_i[j] ~ dnorm(ySuperiorEvap1Bias[m[j]], ySuperiorEvap1Bias_iPrec[m[j]]);
ySuperiorEvap2Bias_i[j] ~ dnorm(ySuperiorEvap2Bias[m[j]], ySuperiorEvap2Bias_iPrec[m[j]]);
ySuperiorRunoff1Bias_i[j] ~ dnorm(ySuperiorRunoff1Bias[m[j]], ySuperiorRunoff1Bias_iPrec[m[j]]);
ySuperiorRunoff2Bias_i[j] ~ dnorm(ySuperiorRunoff2Bias[m[j]], ySuperiorRunoff2Bias_iPrec[m[j]]);
ySuperiorOutflow1Bias_i[j] ~ dnorm(ySuperiorOutflow1Bias[m[j]], ySuperiorOutflow1Bias_iPrec[m[j]]);
ySuperiorOutflow2Bias_i[j] ~ dnorm(ySuperiorOutflow2Bias[m[j]], ySuperiorOutflow2Bias_iPrec[m[j]]);
ySuperiorDiversion1Bias_i[j] ~ dnorm(ySuperiorDiversion1Bias[m[j]], ySuperiorDiversion1Bias_iPrec[m[j]]);

## MICHIGAN-HURON
yMiHuronPrecip1[j] ~ dnorm(yMiHuronPrecip1Mean[j], yMiHuronPrecip1Prec)
yMiHuronPrecip2[j] ~ dnorm(yMiHuronPrecip2Mean[j], yMiHuronPrecip2Prec)
yMiHuronEvap1[j] ~ dnorm(yMiHuronEvap1Mean[j], yMiHuronEvap1Prec)
yMiHuronEvap2[j] ~ dnorm(yMiHuronEvap2Mean[j], yMiHuronEvap2Prec)
yMiHuronRunoff1[j] ~ dnorm(yMiHuronRunoff1Mean[j], yMiHuronRunoff1Prec)
yMiHuronRunoff2[j] ~ dnorm(yMiHuronRunoff2Mean[j], yMiHuronRunoff2Prec)
yMiHuronOutflow1[j] ~ dnorm(yMiHuronOutflow1Mean[j], yMiHuronOutflow1Prec)
yMiHuronOutflow2[j] ~ dnorm(yMiHuronOutflow2Mean[j], yMiHuronOutflow2Prec)
yMiHuronDiversion1[j] ~ dnorm(yMiHuronDiversion1Mean[j], yMiHuronDiversion1Prec)

yMiHuronPrecip1Mean[j] <- miHuronPrecip[j] + yMiHuronPrecip1Bias_i[j]
yMiHuronPrecip2Mean[j] <- miHuronPrecip[j] + yMiHuronPrecip2Bias_i[j]
yMiHuronEvap1Mean[j] <- miHuronEvap[j] + yMiHuronEvap1Bias_i[j]
yMiHuronEvap2Mean[j] <- miHuronEvap[j] + yMiHuronEvap2Bias_i[j]
yMiHuronRunoff1Mean[j] <- miHuronRunoff[j] + yMiHuronRunoff1Bias_i[j]
yMiHuronRunoff2Mean[j] <- miHuronRunoff[j] + yMiHuronRunoff2Bias_i[j]
yMiHuronOutflow1Mean[j] <- miHuronOutflow[j] + yMiHuronOutflow1Bias_i[j]
yMiHuronOutflow2Mean[j] <- miHuronOutflow[j] + yMiHuronOutflow2Bias_i[j]
yMiHuronDiversion1Mean[j] <- miHuronDiversion[j] + yMiHuronDiversion1Bias_i[j]

yMiHuronPrecip1Bias_i[j] ~ dnorm(yMiHuronPrecip1Bias[m[j]], yMiHuronPrecip1Bias_iPrec[m[j]]);
yMiHuronPrecip2Bias_i[j] ~ dnorm(yMiHuronPrecip2Bias[m[j]], yMiHuronPrecip2Bias_iPrec[m[j]]);
yMiHuronEvap1Bias_i[j] ~ dnorm(yMiHuronEvap1Bias[m[j]], yMiHuronEvap1Bias_iPrec[m[j]]);
yMiHuronEvap2Bias_i[j] ~ dnorm(yMiHuronEvap2Bias[m[j]], yMiHuronEvap2Bias_iPrec[m[j]]);
yMiHuronRunoff1Bias_i[j] ~ dnorm(yMiHuronRunoff1Bias[m[j]], yMiHuronRunoff1Bias_iPrec[m[j]]);
yMiHuronRunoff2Bias_i[j] ~ dnorm(yMiHuronRunoff2Bias[m[j]], yMiHuronRunoff2Bias_iPrec[m[j]]);
yMiHuronOutflow1Bias_i[j] ~ dnorm(yMiHuronOutflow1Bias[m[j]], yMiHuronOutflow1Bias_iPrec[m[j]]);
yMiHuronOutflow2Bias_i[j] ~ dnorm(yMiHuronOutflow2Bias[m[j]], yMiHuronOutflow2Bias_iPrec[m[j]]);
yMiHuronDiversion1Bias_i[j] ~ dnorm(yMiHuronDiversion1Bias[m[j]], yMiHuronDiversion1Bias_iPrec[m[j]]);

}

```

```

#####
# Water balance model as described in section 2.1
# Model/Process error follows equation set 5
#####

for(k in rollPeriod:posteriorEndMonth) {
  ### SUPERIOR
  ySuperiorRStore[k] ~ dnorm(superiorRStore[k], ySuperiorRStorePrec)

  superiorRStore[k] <- (
    sum(superiorPrecip[(k-rollPeriod+1):k])
    -sum(superiorEvap[(k-rollPeriod+1):k])
    +sum(superiorRunoff[(k-rollPeriod+1):k])
    -sum(superiorOutflow[(k-rollPeriod+1):k])
    +sum(superiorDiversion[(k-rollPeriod+1):k])
    +sum(superiorProcError_i[(k-rollPeriod+1):k])
  )

  ### MICHIGAN-HURON
  yMiHuronRStore[k] ~ dnorm(miHuronRStore[k], yMiHuronRStorePrec)

  miHuronRStore[k] <- (
    sum(miHuronPrecip[(k-rollPeriod+1):k])
    -sum(miHuronEvap[(k-rollPeriod+1):k])
    +sum(miHuronRunoff[(k-rollPeriod+1):k])
    -sum(miHuronOutflow[(k-rollPeriod+1):k])
    +0.70110653739*sum(superiorOutflow[(k-rollPeriod+1):k])
    -sum(miHuronDiversion[(k-rollPeriod+1):k])
    +sum(miHuronProcError_i[(k-rollPeriod+1):k])
  )
}

#####

## Bias terms, monthly bias precisions, process errors, and monthly
## process error precisions, equation sets 7 and 5 respectively.
## Includes incorporation of expert guidance on Q and D
## They would otherwise have the same bias definition as the other
## variables
#####

for (i in 1:12) {
  ySuperiorPrecip1Bias[i] ~ dnorm(0,0.01)
  ySuperiorPrecip2Bias[i] ~ dnorm(0,0.01)
  ySuperiorEvap1Bias[i] ~ dnorm(0,0.01)
  ySuperiorEvap2Bias[i] ~ dnorm(0,0.01)
  ySuperiorRunoff1Bias[i] ~ dnorm(0,0.01)
  ySuperiorRunoff2Bias[i] ~ dnorm(0,0.01)
  ySuperiorOutflow1Bias[i] ~ dnorm(0,0.25)
  ySuperiorOutflow2Bias[i] ~ dnorm(0,0.25)
  ySuperiorDiversion1Bias[i] ~ dnorm(0,0.25)

  yMiHuronPrecip1Bias[i] ~ dnorm(0,0.01)
  yMiHuronPrecip2Bias[i] ~ dnorm(0,0.01)
  yMiHuronEvap1Bias[i] ~ dnorm(0,0.01)
}

```

```

yMiHuronEvap2Bias[i] ~ dnorm(0,0.01)
yMiHuronRunoff1Bias[i] ~ dnorm(0,0.01)
yMiHuronRunoff2Bias[i] ~ dnorm(0,0.01)
yMiHuronOutflow1Bias[i] ~ dnorm(0,0.25)
yMiHuronOutflow2Bias[i] ~ dnorm(0,0.25)
yMiHuronDiversion1Bias[i] ~ dnorm(0,0.25)

ySuperiorPrecip1Bias_iPrec[i] ~ dgamma(0.05,0.05);
ySuperiorPrecip2Bias_iPrec[i] ~ dgamma(0.05,0.05);
ySuperiorEvap1Bias_iPrec[i] ~ dgamma(0.05,0.05);
ySuperiorEvap2Bias_iPrec[i] ~ dgamma(0.05,0.05);
ySuperiorRunoff1Bias_iPrec[i] ~ dgamma(0.05,0.05);
ySuperiorRunoff2Bias_iPrec[i] ~ dgamma(0.05,0.05);
ySuperiorOutflow1Bias_iPrec[i] ~ dgamma(0.05,0.05);
ySuperiorOutflow2Bias_iPrec[i] ~ dgamma(0.05,0.05);
ySuperiorDiversion1Bias_iPrec[i] ~ dgamma(0.05,0.05);

yMiHuronPrecip1Bias_iPrec[i] ~ dgamma(0.05,0.05);
yMiHuronPrecip2Bias_iPrec[i] ~ dgamma(0.05,0.05);
yMiHuronEvap1Bias_iPrec[i] ~ dgamma(0.05,0.05);
yMiHuronEvap2Bias_iPrec[i] ~ dgamma(0.05,0.05);
yMiHuronRunoff1Bias_iPrec[i] ~ dgamma(0.05,0.05);
yMiHuronRunoff2Bias_iPrec[i] ~ dgamma(0.05,0.05);
yMiHuronOutflow1Bias_iPrec[i] ~ dgamma(0.05,0.05);
yMiHuronOutflow2Bias_iPrec[i] ~ dgamma(0.05,0.05);
yMiHuronDiversion1Bias_iPrec[i] ~ dgamma(0.05,0.05);

superiorProcError[i] ~ dnorm(0,0.01)
miHuronProcError[i] ~ dnorm(0,0.01)

superiorProcError_iPrec[i] ~ dgamma(0.05,0.05);
miHuronProcError_iPrec[i] ~ dgamma(0.05,0.05);
}

#####
## Precision for Observations
#####

### SUPERIOR
ySuperiorRStorePrec ~ dgamma(0.01,0.01)
ySuperiorPrecip1Prec ~ dgamma(0.1,0.1)
ySuperiorPrecip2Prec ~ dgamma(0.1,0.1)
ySuperiorEvap1Prec ~ dgamma(0.1,0.1)
ySuperiorEvap2Prec ~ dgamma(0.1,0.1)
ySuperiorRunoff1Prec ~ dgamma(0.1,0.1)
ySuperiorRunoff2Prec ~ dgamma(0.1,0.1)
ySuperiorOutflow1Prec ~ dgamma(0.1,0.1)
ySuperiorOutflow2Prec ~ dgamma(0.1,0.1)
ySuperiorDiversion1Prec ~ dgamma(0.1,0.1)

### MICHIGAN-HURON
yMiHuronRStorePrec ~ dgamma(0.01,0.01)
yMiHuronPrecip1Prec ~ dgamma(0.1,0.1)
yMiHuronPrecip2Prec ~ dgamma(0.1,0.1)
yMiHuronEvap1Prec ~ dgamma(0.1,0.1)
yMiHuronEvap2Prec ~ dgamma(0.1,0.1)
yMiHuronRunoff1Prec ~ dgamma(0.1,0.1)

```

```

yMiHuronRunoff2Prec ~ dgamma(0.1,0.1)
yMiHuronOutflow1Prec ~ dgamma(0.1,0.1)
yMiHuronOutflow2Prec ~ dgamma(0.1,0.1)
yMiHuronDiversion1Prec ~ dgamma(0.1,0.1)

#####
# Posterior predictive (PP) distributions for verification
#####

for(jp in posteriorStartMonth:posteriorEndMonth) {
  ### SUPERIOR
  ySuperiorPrecip1PP[jp] ~ dnorm(ySuperiorPrecip1Mean[jp], ySuperiorPrecip1Prec)
  ySuperiorPrecip2PP[jp] ~ dnorm(ySuperiorPrecip2Mean[jp], ySuperiorPrecip2Prec)
  ySuperiorEvap1PP[jp] ~ dnorm(ySuperiorEvap1Mean[jp], ySuperiorEvap1Prec)
  ySuperiorEvap2PP[jp] ~ dnorm(ySuperiorEvap2Mean[jp], ySuperiorEvap2Prec)
  ySuperiorRunoff1PP[jp] ~ dnorm(ySuperiorRunoff1Mean[jp], ySuperiorRunoff1Prec)
  ySuperiorRunoff2PP[jp] ~ dnorm(ySuperiorRunoff2Mean[jp], ySuperiorRunoff2Prec)
  ySuperiorOutflow1PP[jp] ~ dnorm(ySuperiorOutflow1Mean[jp], ySuperiorOutflow1Prec)
  ySuperiorOutflow2PP[jp] ~ dnorm(ySuperiorOutflow2Mean[jp], ySuperiorOutflow2Prec)
  ySuperiorDiversion1PP[jp] ~ dnorm(ySuperiorDiversion1Mean[jp], ySuperiorDiversion1Prec)

  ### MICHIGAN-HURON
  yMiHuronPrecip1PP[jp] ~ dnorm(yMiHuronPrecip1Mean[jp], yMiHuronPrecip1Prec)
  yMiHuronPrecip2PP[jp] ~ dnorm(yMiHuronPrecip2Mean[jp], yMiHuronPrecip2Prec)
  yMiHuronEvap1PP[jp] ~ dnorm(yMiHuronEvap1Mean[jp], yMiHuronEvap1Prec)
  yMiHuronEvap2PP[jp] ~ dnorm(yMiHuronEvap2Mean[jp], yMiHuronEvap2Prec)
  yMiHuronRunoff1PP[jp] ~ dnorm(yMiHuronRunoff1Mean[jp], yMiHuronRunoff1Prec)
  yMiHuronRunoff2PP[jp] ~ dnorm(yMiHuronRunoff2Mean[jp], yMiHuronRunoff2Prec)
  yMiHuronOutflow1PP[jp] ~ dnorm(yMiHuronOutflow1Mean[jp], yMiHuronOutflow1Prec)
  yMiHuronOutflow2PP[jp] ~ dnorm(yMiHuronOutflow2Mean[jp], yMiHuronOutflow2Prec)
  yMiHuronDiversion1PP[jp] ~ dnorm(yMiHuronDiversion1Mean[jp], yMiHuronDiversion1Prec)

  # MONTH BY MONTH CHANGE IN STORAGE ANALYSIS

  ySuperiorDStorePP[jp] ~ dnorm(superiorDStore[jp], ySuperiorRStorePrec)

  superiorDStore[jp] <- (
    superiorPrecip[jp]
    -superiorEvap[jp]
    +superiorRunoff[jp]
    -superiorOutflow[jp]
    +superiorDiversion[jp]
    +superiorProcError_i[jp]
  )
  yMiHuronDStorePP[jp] ~ dnorm(miHuronDStore[jp], yMiHuronRStorePrec)

  miHuronDStore[jp] <- (
    miHuronPrecip[jp]
    -miHuronEvap[jp]
    +miHuronRunoff[jp]
    +0.70110653739*superiorOutflow[jp]
    -miHuronOutflow[jp]
    -miHuronDiversion[jp]
  )
}

```

```

        +miHuronProcError_i[jp]
    )
}

### CUMULATIVE STORAGE ANALYSIS

# 1 YEAR

for(x in 12:posteriorEndMonth){
  ySuperiorR1YStorePP[x] ~ dnorm(superiorR1YStore[x], ySuperiorRStorePrec)

  superiorR1YStore[x] <- (
    sum(superiorPrecip[(x-12+1):x])
    -sum(superiorEvap[(x-12+1):x])
    +sum(superiorRunoff[(x-12+1):x])
    -sum(superiorOutflow[(x-12+1):x])
    +sum(superiorDiversion[(x-12+1):x])
    +sum(superiorProcError_i[(x-12+1):x])
  )

  yMiHuronR1YStorePP[x] ~ dnorm(miHuronR1YStore[x], yMiHuronRStorePrec)

  miHuronR1YStore[x] <- (
    sum(miHuronPrecip[(x-12+1):x])
    -sum(miHuronEvap[(x-12+1):x])
    +sum(miHuronRunoff[(x-12+1):x])
    +0.70110653739*sum(superiorOutflow[(x-12+1):x])
    -sum(miHuronOutflow[(x-12+1):x])
    -sum(miHuronDiversion[(x-12+1):x])
    +sum(miHuronProcError_i[(x-12+1):x])
  )
}

# 5 YEAR

for(z in 60:posteriorEndMonth){
  ySuperiorR5YStorePP[z] ~ dnorm(superiorR5YStore[z], ySuperiorRStorePrec)

  superiorR5YStore[z] <- (
    sum(superiorPrecip[(z-60+1):z])
    -sum(superiorEvap[(z-60+1):z])
    +sum(superiorRunoff[(z-60+1):z])
    -sum(superiorOutflow[(z-60+1):z])
    +sum(superiorDiversion[(z-60+1):z])
    +sum(superiorProcError_i[(z-60+1):z])
  )

  yMiHuronR5YStorePP[z] ~ dnorm(miHuronR5YStore[z], yMiHuronRStorePrec)

  miHuronR5YStore[z] <- (
    sum(miHuronPrecip[(z-60+1):z])

```

```

        -sum(miHuronEvap[(z-60+1):z])
        +sum(miHuronRunoff[(z-60+1):z])
        +0.70110653739*sum(superiorOutflow[(z-60+1):z])
        -sum(miHuronOutflow[(z-60+1):z])
        -sum(miHuronDiversion[(z-60+1):z])
        +sum(miHuronProcError_i[(z-60+1):z])
    )
}

# END MODEL

```